Albert-Ludwigs-University Freiburg

Master Thesis

Spatio-temporal interactions between roe deer (*Capreolus capreolus*), Alpine chamois (*Rupicapra rupicapra*) and red deer (*Cervus elaphus*) in the Swiss National Park based on camera traps

---

Author: Luna Emilia Schilli *Matriculation number:* 4741060

A thesis submitted in fulfillment of the requirements for the degree of Master of Science

in the

Chair for Wildlife Ecology and Management

December 7, 2025

Supervisors

Prof. Dr. Ilse Storch
Primary Reviewer, Head of the Chair for Wildlife Ecology and Management, Albert-Ludwigs-Universität Freiburg

Prof. em. Dr. Albert Reif
Secondary Reviewer, Chair of Vegetation Science, Albert-Ludwigs-Universität Freiburg

Dr. Pia Anderwald
External supervisor, Swiss National Park, Research and Monitoring Department

Declaration of Authorship

I, Luna Emilia Schilli, hereby assure that I have written the submitted master's thesis independently, have used no sources or aids other than those indicated , and have identified all content taken literally or in substance from other works as such. The submitted master's thesis is not and has not been the subject of any other examination procedure, either in its entirety or in substantial parts. The online translator DeepL was used for partial text translation and language improvement (DeepL, 2025). The OpenAI software ChatGPT was used to assist with R code debugging, plot adjustment, and LaTeX formatting. All outputs were checked and validated by the author.

Signed:

_____

Date:

_____

ALBERT-LUDWIGS-UNIVERSITY FREIBURG

Abstract

Faculty for Environment and Natural Resources
Chair for Wildlife Ecology and Management

Master of Science

Spatio-temporal interactions between roe deer (*Capreolus capreolus*), Alpine chamois (*Rupicapra rupicapra*) and red deer (*Cervus elaphus*) in the Swiss National Park based on camera traps

by Luna Emilia Schilli

Interactions between species can influence and alter their use of space, activity patterns or food intake. Such interactions can lead to avoidance or displacement mechanisms, particularly between species at the same trophic level with similar habitat requirements. In alpine regions, possible interactions between three of the four most common ungulate species - red deer, roe deer and chamois - have been little studied, although red deer have been observed to be the dominant ungulate species in many ecosystems compared to smaller or more specialised species.

The present study addresses this knowledge gap. Using multi-scale camera trap event data from the the Swiss National Park, possible spatial and temporal interactions between the species were investigated. For this purpose, Generalized Linear Mixed Models with the presence of one species as the dependent variable were conducted. Possible influencing factors were the presence of other species and environmental variables in order to determine spatial segregation. In addition, a directed interval analysis between events of the three species was carried out. The Generalized Linear Mixed Models included the intervals between events of one species pair as the dependent variables. Possible influencing factors were the species pair direction (A $\rightarrow$ B or B $\rightarrow$ A) and environmental variables. Hereby, it was analysed whether roe deer and chamois avoid red deer temporally, i.e. whether the intervals after a red deer detection are longer than vice versa.

The spatial distribution of all three species was primarily determined by environmental gradients and resource availability; there was no evidence of spatial displacement of roe deer or chamois by red deer. The temporal interval analyses, on the other hand, showed asymmetrical interactions: roe deer and chamois occurred at longer intervals after red deer detections than vice versa, indicating temporal avoidance reactions. Overall, competitive processes occur primarily in time rather than space, suggesting behaviourally mediated coexistence without spatial segregation. The findings are directly relevant for multi-species monitoring approaches in topographically restricted alpine systems and provide starting points for the management of ungulates under changing environmental conditions.

Acknowledgements

First and foremost, I would like to express my sincere gratitude to Dr. Pia Anderwald for excellent supervision, continuous and appreciative support, and constructive feedback throughout the entire process of this thesis.

I also thank Prof. Dr. Ilse Storch for supporting the search for the thesis topic, for giving me the opportunity to visit and get to know the Swiss National Park, and for the helpful guidance during the course of this work. I am furthermore thankful that Prof. Dr. Albert Reif agreed to act as second examiner, thereby making this thesis possible in the first place.

I also wish to thank the Swiss National Park for providing the camera-trap and geodata that form the basis of this study.

Contents

List of Figures

List of Tables

Chapter 1

Interspecific interactions between herbivores

Interactions between different species can influence ecological processes and population dynamics (Schoener, 1973). They are fundamental drivers of community dynamics and resource partitioning among herbivores (De Boer and Prins, 1990). They range from positive interactions, such as facilitation or commensalism, to antagonistic processes such as competition and predation (Schoener, 1973; Krebs, 2001). Krebs (2001) defines five types of interactions in animal communities. These include mutualism and commensalism, in which at least one of the species benefits without harming the other, and parasitism, predation, and competition, which harms at least one of the species.

The various forms of competition can be classified into exploitative or interference competition (Holdridge et al., 2016). Exploitative competition is indirect through shared limited resources, and therefore dependent on resource availability. Interference competition prevents access to resources directly through aggressive or passive behaviour, but is not dependent on resource availability (Holdridge et al., 2016). In practice, interference or exploitative competition are often difficult to distinguish (Holdridge et al., 2016).

Among herbivores, interactions can be complex, ranging from facilitative mechanisms to direct competition. De Boer and Prins (1990) have defined the possible interactions between herbivores more precisely. Three different mechanisms can occur in the case of mutual or unilateral benefit. In the case of facilitation, different grazers benefit from each other by, for example, making food more accessible to the other species through their feeding behaviour. In the food manipulation strategy, interspecific competition is avoided by cyclic migration so that the best vegetation status for each species is maintained. The third point is predator detection and protection, where several herbivore species stay in the same area to protect or warn each other against predation.

Conversely, other conditions may result in competition, which often leads to reduced fitness of the inferior competitor. According to De Boer and Prins (1990), interspecific competition can occur if habitat requirements of the different species overlap, they have overlapping feeding behaviour, and the availability of food and resources is limited. This can lead to a reduction in fecundity, growth or survival of the inferior or both of the competitors (De Boer and Prins, 1990; Parker et al., 2009). This type of competition can be inferred when an increase in the population size of one species coincides with a decline in another within the same area, but not when the species occur separately (De Boer and Prins, 1990).

Species can reduce such competition and promote coexistence through niche partitioning, which may occur along spatial or temporal axes (Schoener, 1973; Durant, 1998; Darmon et al., 2012), whereby niche defines the conditions and resources needed for and/or impacting a species to persist (Gillespie, 2024). Therefore conversely, niche

partitioning does not necessarily indicate competition. In the case of habitat overlap, a small overlap with similar requirements can also speak in favour of strong competition, while complete overlap can be an indicator of functioning coexistence as no niche partitioning seems to be necessary or there is no limitation of resources. No overlap is also not necessarily an indication of competition if species generally have different habitat requirements (Schoener, 1973; De Boer and Prins, 1990; Darmon et al., 2012; Corlatti et al., 2019). Conclusively, niche partitioning alone does not have to be an indicator for competition, but competition often manifests itself in different spatial and/or temporal distributions (niche partitioning) to effectively avoid a dominant species (Schoener, 1973; Durant, 1998). Spatial and temporal segregation therefore represent specific forms of niche partitioning that facilitate coexistence among species with overlapping ecological requirements.

Spatial niche partitioning can occur at different scales, from habitat segregation at the landscape level to microhabitats or feeding site selection (Cromsigt and Olff, 2006). This can be particularly evident between species with similar habitat requirements. For example, inferior species such as roe deer (*Capreolus capreolus*) are often found outside protected areas because the number of competing ungulate species is usually lower there (Borkowski et al., 2021). Particularly in direct competition with the generalist, physically larger red deer (*Cervus elaphus*), spatial displacement or avoidance mechanisms were found in roe deer (Torres et al., 2012; Borkowski et al., 2021). The same applies to chamois (*Rupicapra rupicapra*), whose habitat use has been altered by red deer numbers, possibly resulting in a decline in fitness for parts of the population (Anderwald et al., 2016)

Temporal partitioning, involves the segregation of species in time, for instance by shifting diel activity or seasonal use of shared habitats (Schoener, 1973; Durant, 1998; Darmon et al., 2012; Smith et al., 2023). In the absence of spatial partitioning, species can avoid each other temporally in the same areas. Such temporal partitioning has been studied both between predator and prey species (Šprem et al., 2015; Marshall et al., 2023) and between species of the same trophic level (Di Bitetti et al., 2010; Šprem et al., 2015; Kavčić et al., 2021; Marshall et al., 2023; Smith et al., 2023). One can either identify general shifts in diurnal patterns (Šprem et al., 2015; Kavčić et al., 2021; Smith et al., 2023), or determine the intervals between the appearance of one species and the appearance of the next species at the same location (Marion et al., 2022; Marshall et al., 2023; Smith et al., 2023). In the case of species-pair-specific differences, a longer interval between species A to species B than vice versa can indicate possible avoidance or displacement of B by A (Niedballa et al., 2019). Therefore, temporal segregation may be detected at coarse or fine temporal scales even if there is no spatial segregation.

Furthermore, patterns of spatial and temporal segregation are not static; they are strongly modulated by short-term weather and microclimate, as well as forage quality. For example, forest stands can buffer thermal stress and attenuate heavy rainfall (de Frenne et al., 2019; van Beest et al., 2012; Anderwald et al., 2024), whereas in the absence of heat waves, storms, or prolonged rain, open habitats often provide good grazing opportunities (Johnson et al., 1995; Brivio et al., 2019; Widén et al., 2025). In summer, Alpine chamois (*Rupicapra rupicapra*) also mitigate heat exposure by selecting cooler, north-facing aspects and, during heavy rainfall, can shift to lower elevations (Anderwald et al., 2024). Roe deer are less susceptible to heat stress (Widén et al., 2025) and generally spend more time in denser wooded habitats compared to red deer. These context-dependent shifts create temporal windows in which species either segregate (seeking thermal/refuge habitats) or overlap (tracking high-quality forage), shaping the strength and detectability of interspecific interactions, and therefore should

be considered in respective analysis.

Different approaches have been developed to quantify spatial and temporal partitioning, depending on study scale and target species. Previous studies have used a wide variety of monitoring methods, such as the scan method (Anderwald et al., 2015), GPS data (Anderwald et al., 2024) or camera trap data (Sollmann, 2018; Donini et al., 2025). Camera traps offer the advantage of being non-invasive and allowing multiple species to be monitored simultaneously over long periods of time at many locations (Burton et al., 2015; Sollmann, 2018). Diurnal overlap, spatial use based on presence data of various types, partial group size, or animal demographics can all be inferred from such studies. Based on this sort of camera trap data, for example, Smith et al. (2023) and Marshall et al. (2023) observed temporal segregation of detections of potentially competing species in the absence of spatial segregation. Studies such as Marion et al. (2022) or Donini et al. (2025) demonstrate the usefulness of camera traps for detecting spatial distribution patterns of herbivores that may indicate displacement or avoidance. In particular, combining both spatial and temporal partitioning patterns within a single study provides the most comprehensive picture possible for underlying interspecies interactions, which is why many studies combine both approaches in their methodology (Marion et al., 2022; Donini et al., 2025).

In this study, spatial and temporal segregation between three ungulate species from the Swiss National Park will be analysed based on camera trap data. The three species studied are red deer (*Cervus elaphus*), roe deer (*Capreolus capreolus*) and Alpine chamois (*Rupicapra rupicapra*). They show overlapping habitat requirements, and different types of competition (mainly exploitative) between red deer and the other two species have been observed in previous studies in the Swiss National Park and in other areas (Anderwald et al., 2015, 2016; Corlatti et al., 2019; Ferretti et al., 2019; Borkowski et al., 2021; Donini et al., 2025). As red deer populations have widely recovered, interspecific interactions have been studied in many protected areas. Because ungulate densities there often exceed those in adjacent or hunted regions, these sites are especially suitable for investigating potential interactions (Wagner et al., 2006; Borkowski et al., 2019). The Swiss National Park is a suitable study area for such analyses due to its large ungulate populations, absence of hunting and topographic diversity.

1.1 Interspecific interactions between red deer (*Cervus elaphus*) and roe deer (*Capreolus capreolus*)

As a smaller species with browser feeding habits, roe deer are often at a competitive disadvantage compared to other ungulates in potential competitive situations. In many studies on interactions between roe deer and other ungulates, roe deer were negatively influenced by other species such as muntjac (*Muntiacus* spp.,Hemami et al. (2005)) or fallow deer (*Dama dama*, Ferretti et al. (2008)). As two of the most common cervids in Europe (Apollonio et al., 2010), the possible interactions between red deer and roe deer are particularly important to investigate. Roe deer and red deer show large overlap in their habitats (Apollonio et al., 2010; Borkowski et al., 2021) and partial overlap in their choice of food (Latham et al., 1999), whereby the larger red deer with a broader food niche also accesses all dietary resources of the smaller roe deer as a selective feeder, but not vice versa (Storms et al., 2008; Mancinelli, S. et al., 2015). Latham et al. (1996) observed a negative influence of red deer on roe deer numbers in Scotland. With regard to spatial distribution, Torres et al. (2012) and Borkowski et al. (2021) have shown that roe deer can be spatially displaced by higher red deer

numbers. One of the few studies on red and roe deer interactions in the Alps on a spatial and temporal scale is Donini et al. (2025) from the Stelvio National Park. Here, no significant correlation was found between red deer abundance and the probability of roe deer occupancy, and there was no temporal adjustment regarding diel activity (Donini et al., 2025).

Based on the available literature, I hypothesize that the spatial distribution of roe deer should be influenced by the presence of red deer. On the other hand, there is no evidence so far for temporal segregation between the two species, especially in alpine areas. The hypotheses are therefore:

Hypothesis H1 (Spatial segregation roe deer)**.** *Roe deer presence is negatively influenced by red deer presence at the same camera location within 24 hours.*

Hypothesis H2 (Temporal segregation roe deer)**.** *Roe deer do not temporarily avoid sites with previous abundance of red deer. Therefore, intervals between roe deer to red deer detections are not significantly shorter than from red deer to roe deer detections.*

1.2 Interspecific interactions between red deer (*Cervus elaphus*) and Alpine chamois (*Rupicapra rupicapra*)

Due to the large dietary overlap between chamois and red deer as intermediate feeders (Lovari et al., 2014; Andreoli et al., 2016) and overlapping habitat requirements, competition between chamois and red deer can occur (De Boer and Prins, 1990; Lovari et al., 2014; Andreoli et al., 2016; Corlatti et al., 2019; Ferretti et al., 2019; Kavčić et al., 2021). In the Stelvio National Park in the Italian Alps, Corlatti et al. (2019) found negative demographic consequences on chamois populations due to the increase of red deer numbers in the same area. The population growth of chamois was mostly influenced by the red deer population size in the previous year (Corlatti et al., 2019). Anderwald et al. (2015) and Anderwald et al. (2016) investigated the influence of red deer on habitat utilisation, population growth, and/or the body condition of individuals measured by horn growth in the Swiss National Park. Red deer abundance had no influence on the population growth of chamois, but an effect on horn growth of young animals and habitat utilisation. In the two areas studied, different levels of segregation between chamois and red deer were observed (Anderwald et al., 2015, 2016). Ferretti et al. (2019) support these results. They found interspecific competition between Appenine chamois (*Rupicapra pyrenaica ornata*) and red deer. The negative impact of red deer was exacerbated by changing weather conditions. As the Appenine chamois is vulnuerable to extinction, this is an important observation, especially with regard to climate change (Lovari et al., 2014; Ferretti et al., 2019). Thus, possible negative consequences of climate change on chamois can be exacerbated by the increased presence of red deer at higher elevations (Willisch et al., 2013; Ferretti et al., 2019). Kavčić et al. (2021) found a temporal decoupling between red deer and chamois presence and their temporal overlap during the day. As the effects were only weak, they indicated that further studies with a larger sample size and smaller spatial resolution were needed (Kavčić et al., 2021). These results show possible patterns of interspecific competition between red deer and chamois. This is particularly relevant as competition at the same trophic level leads to ecological niche partitioning such as spatial or temporal segregation (Darmon et al., 2012), which is the aim of the present study.

Based on the available literature, I hypothesize that the spatial distribution of chamois should be influenced by the presence of red deer, and that temporal segregation between the two species should occur during the summer period.

Hypothesis H3 (Spatial segregation chamois)**.** *Chamois presence is negatively influenced by red deer presence at the same camera location within 24 hours, leading to spatial segregation between the two species.*

Hypothesis H4 (Temporal segregation chamois)**.** *Chamois temporarily avoid sites with previous presence of red deer. Intervals from red deer to chamois detections should therefore be significantly longer than vice versa, indicating one-sided temporal segregation.*

Chapter 2

Methods

2.1 Study area and data collection

The study is based on data from the Il Fuorn area located in the northern part of the Swiss National Park in the Central Alps (46.66° N, 10.2° E). The study area is located at 1800-2800 m above sea level and is characterised by a continental climate. Consequently, there is continuous snow cover from November to the end of April, and the vegetation period lasts from June to the end of September. The main habitat types are alpine and subalpine grassland, coniferous forest and scree and rocks (in the following: bare ground) (Zoller, 1995).

In the Il Fuorn area of the Swiss National Park, ungulate numbers fluctuated between 392-520 chamois and 421-491 red deer between 2018 and 2021 (Schweizerischer Nationalpark, 2019, 2020, 2021). Newly published roe deer numbers of 2.34 roe deer/ km^2 (Timcke, 2025) were not yet available in previous evaluations. Red deer are only resident in the National Park area during the summer months (from June to October). In autumn, they migrate to lower areas to spend the winter outside the National Park (Haller, 2002; Anderwald et al., 2015, 2016). In these wintering areas, the red deer population is controlled by culling (Anderwald et al., 2015). In contrast to migratory red deer, chamois and roe deer populations are not directly controlled by humans (Anderwald et al., 2015, 2016). The presence of predators during the study period was limited to individual wolves migrating through and a single resident wolf (*Canis lupus*) (Schweizerischer Nationalpark, 2019, 2020, 2021). Predators were therefore not specifically taken into account.

The Swiss National Park was founded in 1914, making it the oldest National Park in the Alps. It is also the only National Park in Switzerland and has the highest protection status 1a (wilderness area) according to the International Union for Conservation of Nature (IUCN) (IUCN, 2025). This status protects natural processes of habitats, animals and plants from human intervention. There is no hunting in the National Park area and anthropogenic disturbance is minimized by enforcing strict rules (e.g. visitors have to keep to trails and cannot bring dogs to the park). During winter and at night, the park is closed to visitors (Schweizerischer Nationalpark, 2024). One of the main objectives of the National Park is research. There are many long-term monitoring and research projects in the park to investigate natural processes taking place without human disturbance (Schweizerischer Nationalpark, 2024).

2.1.1 Data and data preparation

Statistical analyses and data preparation were carried out with RStudio Version 4.1.2 and 4.5.0 (R Core Team, 2021). The map in Figure 2.1 was created with QGIS Version 3.42 Muenster (QGIS Development Team, 2025). The online translator DeepL was used for partial text translation and language improvement (DeepL, 2025). The OpenAI

software ChatGPT was used to assist with R code debugging, plot adjustment, and LaTeX formatting. All outputs were checked and validated by the author.

Camera data

Since 2018, a camera trap network has been established in the park for monitoring purposes mainly during the vegetation period. Due to the risk of avalanches, ca. one third of the cameras, particularly on the 1 km grid, had to be removed during the remaining months. However, as red deer are only present in the park during the vegetation period, the surveys were limited to the beginning of July to the end of September in 2018, 2019, 2020 and 2021. At all locations, the camera used was a Bushnell Trophy Cam HD Aggressor 119876 camera trap. It was set to capture single images with low sensor sensitivity and a short trigger interval (single-shot mode, sensitivity: low, interval: 0.6 s). The infrared flash and night vision operated automatically at high LED intensity (IR flash: high, night shutter: auto), and images were recorded at high resolution (5920×3416 pixels, 38° angle of view).

The camera data originates from two separate camera grids: one at a resolution of 1 km, the other at 250 m, whereby the 250 m grid was embedded in the larger 1 km grid and was specifically set up to monitor roe deer in the National Park area (Figure 2.1).

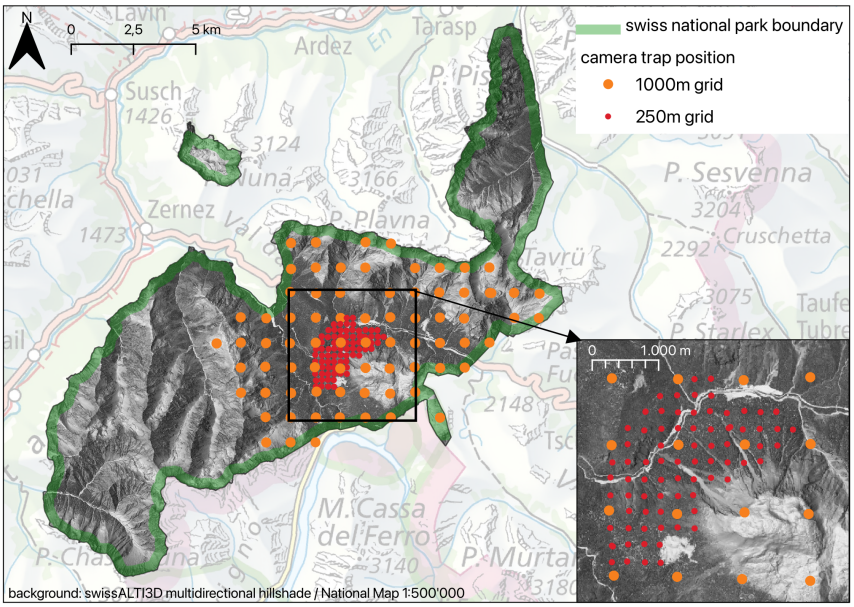

Figure 2.1: General camera trap locations on the 250 m (red) and 1 km (yellow) grids, background from Federal Office of Topography (swisstopo) (2024a,b)

Locations of individual cameras have not changed over the years. The images were processed by park staff in two semi-automated steps and summarised in a data set divided into events. Images of the same species that were less than 5 minutes apart or validated to detect the same individual (e.g. sleeping) were summarised as one event. Each event was given an event ID and a start and end time with a duration of zero if only one image was taken during this event. Each event also contains the respective location (EPSG:2056) on the grid and an estimate of the group size if several individuals of one species were detected at the same time.

To limit the study period to the time when all three species were present in the study area, camera data were limited to the period between June and September. As cameras at higher elevation and thus other habitats (e.g. bare ground) can only be set

up later in the year, the analysis only started when 95 % of the cameras were set up in each year (for detailed study periods see Table 2.1). This also took into account the habitat preference of the species, as fewer cameras at higher elevation outside the forest could cause a bias in chamois detections. They spend less time in forests and at lower elevations than red deer and roe deer (Anderwald et al., 2024), which reduced their detection probability if an insufficient number of cameras were running above the treeline. Cameras that had an error for more than 30 days within the study period were completely excluded from the analysis for that year. In addition, data from some cameras was not fully processed in some years. These were also removed from the data set in the respective year. Confirmed problem periods of less than 30 days were deducted from the trapping days of each camera to keep the detection effort realistic, resulting in the random factor 'trap days' used in the models.

Table 2.1: Duration of time spans with at least 95% of cameras active, resulting in the respective study period per year and the number of cameras included.

Year	Starting date	Ending date	Trapdays	1 km grid	250 m grid
2018	11.07.2018	10.09.2018	62	68	73
2019	11.07.2019	12.09.2019	64	73	75
2020	06.07.2020	15.09.2020	72	69	73
2021	05.07.2021	13.09.2021	71	72	74

All subsequent analyses were based on events from the 1 km grid and the 250 m grid. In total, I analyzed $n = 11{,}579$ events from the 1 km grid and $n = 16{,}373$ events from the 250 m grid across the four-year study period. Events were mostly evenly distributed across years and grids. There were less roe deer detections compared to the other two species, especially on the 1 km grid. Red deer were detected most (Table 2.2).

Table 2.2: Number of camera-trap events per species, year and grid.

Species	Year	1 km	250 m
Roe deer	2018	135	421
Roe deer	2019	232	768
Roe deer	2020	213	647
Roe deer	2021	208	535
Chamois	2018	1110	908
Chamois	2019	1276	940
Chamois	2020	1243	1093
Chamois	2021	1181	1067
Red deer	2018	1279	2146
Red deer	2019	1637	2416
Red deer	2020	1709	2869
Red deer	2021	1356	2563

Environmental data

In addition to this camera data, environmental and weather variables were included to control for additional possible influencing factors on species presence and distribution (MacKenzie et al., 2004; Ramesh et al., 2017). To test for topography variables a

digital terrain model of the Swiss National Park at 0.5 m resolution was available (Federal Office of Topography (swisstopo), 2024c). The digital terrain model contained information of elevation, and derived from this, slope and aspect at each location. Prior to analysis, each event was assigned the slope, elevation and aspect at its location. Using `terra::terrain` in R (Hijmans, 2025), slope and aspect were calculated as a grid from the digital terrain model (`unit = 'degrees'`) and then extracted individually for each location. Aspect (0-360 °) was transformed to radians and split into northness = cos(Aspect) and eastness = sin(Aspect), i.e. two linear variables for modelling purposes.

A map of the habitat types in and around the park (Lotz, 2006) contained categorical information of the dominant habitat type. Habitat types were grouped into three main categories based on the dominant land cover: meadows, bare ground/ sparsely vegetated areas, and forests. For each location the respective habitat type got extracted. As stated in the introduction, habitat use by ungulates can change, particularly in response to extreme weather events. For this reason, weather data was included in both the spatial and temporal analysis in addition to location variables.

Hourly and daily weather data from Buffalora (station BUF; 46.648408° N, 10.2672° E) were used, including daily air temperature averages, daily temperature maxima and minima, as well as hourly and daily sum of precipitation (Federal Office of Meteorology and Climatology MeteoSwiss, 2025). As weather data came from one single weather station right outside the park borders, precipitation and temperature did not differ between camera locations. To test for seasonality effects, Julian day (day of year 1–365, or 1–366 in leap years) was calculated for each event.

2.1.2 Statistical analysis

Generalized linear mixed models (GLMM) were used to analyse possible displacement patterns without performing specific density calculations for each species (Sollmann, 2018). They were conducted by using the R-package `glmmTMB` (Brooks et al., 2017). Camera location and actual trap days per camera were included as random factors into the models (Nakagawa et al., 2017; Burton et al., 2015). The three species were tested against each other to detect possible interactions in any direction. GLMMs were deliberately chosen over occupancy models because the focus was on relative use and interaction effects at individual locations. In addition, key effort and detection covariates as well as random effects at the location level were taken into account. Moreover, all cameras were of the same model with identical settings. Detection differences are therefore more likely to be of natural origin, such as habitat type, but these were included in the model (MacKenzie et al., 2002, 2004). Although occupancy models better separate the ecological from the observational process, GLMMs were appropriate here in terms of study design and objectives.

To assess potential collinearity among predictors, pairwise Spearman rank correlations were calculated using the `cor(method="spearman")` function in R. Correlation matrices were inspected, and a threshold of $|r| > 0.7$ was defined as a critical level of collinearity that may affect model stability (Dormann et al., 2013). In order to avoid collinearity, only one level (daily or hourly) of temperature and precipitation was included for each model. Weather covariates were selected to match the temporal scope of the study. For the spatial analysis, which was based on 24-hour slots, the maximum daily temperature and total precipitation within 24 hours were used. In the temporal analysis, which considered the dynamic direct intervals between events, precipitation and the current temperature at the time of the initial event were taken into account. This avoided the only source of collinearity between different weather

variables, and none of the other predictors showed significant collinear relationships (>0.7). The habitat categories were an exception, as they showed a high correlation because they each belong to one factor variable as dummy codes and there was a correlation between sin(time) and temperature. Since the latter correlation value was directly at 0.7 and both effects were considered important individually, both variables were retained in the model (Correlation matrices Appendix B).

Spatial analysis

To determine possible spatial partitioning, the event data for each site were summarized as a presence-absence dataset for each species and location every 24 hours.

All relevant continuous predictors were z-transformed, including 24-hour sum of precipitation, maximum and minimum temperature, Julian day, elevation and slope. Additionally, the 24-hour precipitation value was log-transformed to minimize right skewness. The categorical variables (competitor presence and habitat type) were dummy coded. The data were then split based on grid type. For each species and grid type, a binomial GLMM was fitted. The fixed effects were the presence of the two competitor species, habitat type, weather variables (24-hour precipitation and minimum and maximum temperature), Julian day, and topography variables (elevation, slope, northness and eastness). Random intercepts for locationID, and sampling effort (trapdays) were included for each camera, resulting in the following model structure.

$$Y_{\text{Species A},i} \sim \text{Binomial}\big(n_i,\ p_{\text{Species A},i}\big)$$

$$\begin{aligned}\text{logit}(\Pr(\text{SpeciesA}_i = 1)) = {} & \beta_0 + \beta_1 \cdot \text{northness}_{z,i} + \beta_2 \cdot \text{eastness}_{z,i} \\ & + \beta_3 \cdot \text{elevation}_{z,i} + \beta_4 \cdot \text{Julian\_day}_{z,i} + \beta_5 \cdot \text{precip24h\_log}_{z,i} \\ & + \beta_6 \cdot \text{presence}_{\text{Species B},i} + \beta_7 \cdot \text{Habitat type}_i + \beta_8 \cdot \text{slope}_{z,i} \\ & + \beta_9 \cdot \text{max\_temp}_{z,i} + \beta_{10} \cdot \text{min\_temp}_{z,i} + \beta_{1_1} \cdot \text{presence}_{\text{Species C},i} \\ & + u_{\text{Location}[i]} + v_{\text{trap days}[i]}\end{aligned}$$

with A, B, C species placeholders, i the 24-hour slot, n_i the binomial trials, $p_{\text{Species A},i}$ the presence of Species A, Habitat type$_i$ the habitat category, $u_{\text{Location}[i]} \sim \mathcal{N}(0, \sigma_L^2)$ the random intercept for camera location, and $v_{\text{trapdays}[i]} \sim \mathcal{N}(0, \sigma_T^2)$ the random effect for trapdays.

In addition, I used the likelihood ratio test and Akaike Information Criterion corrected for small sample sizes (AICc) (Akaike, 1973; Symonds and Moussalli, 2011) to test for biologically plausible interactions between the presence of the potentially competing species and precipitation and Julian day (Precipitation x Species presence and Julian day x Species presence) (MacKenzie et al., 2004; Ramesh et al., 2017; Tallian et al., 2022). For the biological background for the two interactions used see Appendix A. These variables are expected to modulate species responses with changing weather and environmental changes during the study period. I did not fit the full set of all possible interactions to avoid overparameterization. For each species and grid, I fitted a set of candidate global models: one without interaction terms and additional models including each of the two candidate interactions. The interaction was included into the global model if the model including this interaction (i) had the lowest AICc among the candidate models and (ii) the interaction itself was statistically significant ($p < 0.05$; Akaike, 1973; Symonds and Moussalli, 2011). This resulted in six global

models, which were validated by checking distributional assumptions using the `DHARMa` package (Hartig, 2024). Both statistical and visual checks were performed to assess residual uniformity (via the Kolmogorov–Smirnov test), dispersion, and zero-inflation, whereby visual checks were deemed to be more important for substantial model fit (Hartig, 2024).

The validated global models were ranked by using the `dredge::MuMIn` package (Bartoń, 2025) across all fixed effects. Top candidate GLMMs were ranked using AICc (Akaike, 1973; Symonds and Moussalli, 2011). Models with $\Delta\text{AICc} \leq 2$ (relative to the minimum AICc) were deemed to have substantial empirical support (Burnham and Anderson, 2004; Symonds and Moussalli, 2011; Richards et al., 2011; Ramesh et al., 2017). Since none of the Top models had sufficient Akaike weight (Table 3.1), indicating model selection uncertainty, an averaged model was created from these remaining models (Arnold, 2010; Symonds and Moussalli, 2011).

The relative importance of individual predictors was calculated from this averaged model by summing up Akaike weights (w^+) across all models in which the predictor was included (Burnham and Anderson, 2004; Arnold, 2010; Symonds and Moussalli, 2011). If a predictor is included in all or many Top models, the summed Akiake weight approaches 1.0. The value decreases as the number of models in which it is included decreases. From this, a tendency can be derived as to whether the predictor has a high probability of belonging to the best model. This was a further precautionary measure to avoid overinterpreting parameters with little explanatory power (Arnold, 2010).

The direction and strength of predictor effects were described by the model-averaged estimate $\hat{\beta}$. The significance or further relevance of the effects was assessed using the 95% confidence intervals (95% CI) based on conditional standard errors (`revised.var = TRUE`, `unconditional = FALSE`). If the 95% CI excluded 0, a robust significant effect was inferred across the models; if it included 0, the effect was classified as uncertain or inconsistent (exemplary comparable method in Ngoprasert et al. (2022); Tallian et al. (2022); Semper-Pascual et al. (2023)).

The averaged coefficients from the averaged model were used as the basis for predictions. For effect plots, marginal predictions were obtained from the GLMMs on the link scale (using fixed effects only), and then back-transformed to the response scale using the appropriate inverse link function. Uncertainty bands of ± 1 standard error (± 1 SE) were approximated on the response scale using the Delta method applied to the back-transformed predictions (Nakagawa et al., 2017; Lenth, 2025a,b). All plots were produced in `ggplot2` (Wickham, 2016), with covariates expressed in their original units by inverting the underlying z-scaling (from the data mean and standard deviation or the attributes stored by `scale()`, Schielzeth (2010)) .

Due to the biology and data availability on roe deer and chamois, the group size per event resulted in too little variance, which is why only presence-absence data were evaluated, as described above. However, if there were significant effects of red deer presence in a model, one additional model with red deer count as a predictor was included, to test for possible effects of the group size of red deer. The model evaluation procedure was the same as for the presence-absence models.

Temporal analysis

To assess the behavioral avoidance between different species by using the time-to-event analysis, a GLMM with the temporal intervals between events was performed. A before/after occurrence (e.g. red deer (before)→roe deer (after), roe deer (before)→red deer (after)) for the detected species was used (Sollmann, 2018; Niedballa et al., 2019; Marion et al., 2022; Marshall et al., 2023; Smith et al., 2023). For each event, the

minimum time to each subsequent event was determined between all species pairs at each camera location in each study period (Sollmann, 2018; Marshall et al., 2023). If the start time of the subsequent event was before the end time of the previous event, it indicated overlap between events and the interval was set to 0 (n=43 = 0.095%). Because this extremely small proportion led to modelling issues in the GLMM and would have required a separate modelling framework (e.g. a hurdle or zero-inflated model; Brooks et al., 2017) that was not justified by the low sample size, 0-values were excluded from the interval analysis.

The time of day for each event was converted into two linear variables (Donini et al., 2025). The timestamp of each detection was converted into radians with the calculations given below and then broken down into its sine and cosine components (Donini et al., 2025).

$$\begin{aligned} \text{time}_{\text{rad}} &= 2\pi \cdot \left(\frac{\text{Hour} \cdot 3600 + \text{Minute} \cdot 60}{86400} \right) \\ \sin\_\text{time} &= \sin(\text{time}_{\text{rad}}) \\ \cos\_\text{time} &= \cos(\text{time}_{\text{rad}}) \end{aligned}$$

These two variables (`sin(time)` and `cos(time)`) were integrated into the GLMM as covariates to capture diurnal activity patterns. As in the spatial analysis, environmental and location variables (habitat, slope, elevation) (Ramesh et al., 2017), as well as weather (precipitation per hour and hourly temperature), were also included in the model as z-scaled covariates (Niedballa et al., 2019). Location and year were added as random factors. Precipitation was log-transformed to handle strong right-scewness. Northness and eastness were excluded from the models, as they did not have a significant effect in the spatial analysis and caused problems during model selection.

GLMMs with the `glmmTMB` function (Brooks et al., 2017) were used to model the temporal intervals (`interval_min`) between species pairs. The `glmmTMB` package was used for the possibility of dealing with different variances between the predictors by using a separate variance model (`dispformula`). A separate model was processed for each species pair, containing the interval direction of the species combination ($A \rightarrow B$ and $B \rightarrow A$). In all cases, Gamma models with log link provided the best residual distribution in visual `DHARMa` checks (Hartig, 2024).

To account for heterogeneity in the variances between predictor values, alternative dispersion terms were specified setting `dispformula` (Brooks et al., 2017). Various candidate models with dispersion as a function of species pair, habitat type, elevation, and Julian day were tested and compared using AICc. The best Gamma model with the lowest AICc was used as the global model for further model selection (Table 3.2) (Akaike, 1973; Symonds and Moussalli, 2011). No interaction terms were tested, as overparameterization was to be avoided due to the smaller sample in the temporal analysis. Model validation and selection were performed using visual `DHARMa` diagnostics within the `MuMIn` package, as in the spatial analysis (Bartoń, 2025).

For the 250 m grid (red deer ↔ chamois), the model diagnostics showed systematic deviations, and the residuals against fitted values showed pronounced trends. The 250 m design was primarily set up to record roe deer in forested areas; accordingly, the habitat distribution for red deer and chamois is highly unbalanced. Together with the scale mismatch (250 m grid vs. typical movement intervals of red deer/chamois), the data do not meet key model assumptions. For these reasons, red deer ↔ chamois on the 250 m grid was excluded from the main analysis and the evaluation was limited to the 1 km grid (and comparisons suitable for roe deer).

The procedure for calculating effect sizes and converting them back to the original scale was identical to that used in spatial analysis.

Chapter 3

Results

For both spatial and temporal analysis, overlapping potential factors influencing species distribution were included in the models. However, only the spatial analysis tested for northness and eastness. In the temporal analysis, two additional predictors to test for diel activity were included. The effect of a covariate was considered significant when the 95% CI did not overlap zero (dashed vertical lines in forest plots). Coefficients (β) reported in the Results are on the link scale (logit for presence models, log for temporal intervals) and refer to a 1 standard deviation (1 SD) change. The model results of the model averaging are presented below by species and by grid. The text focuses in particular on significant effects; effect sizes and 95% CI of the non-significant effects can be taken from the respective forest plots.

3.1 Spatial analysis

Each averaged model included all environmental and weather variables. The presence data of other species were only included in some of the averaged models and the species differed between each model (Table 3.1).

Table 3.1: Model-averaged spatial GLMMs. Formulas show the fixed effects across the respective Top models; all models include random intercepts for `location` and `number of trap days`. Weight and ΔAICc ranges refer to the models included (Top) in the corresponding Top-model set.

Model	Model (averaged; formula incl. random effects)	Top	Weight	ΔAICc
Chamois (1 km)	Chamois_pres ∼ eastness_z + northness_z + elevation_z + julian_day_z + slope_z + precip24h_log_z + Red_deer_pres + precip24h_log_z:Red_deer_pres + max_temp_z + min_temp_z + Roe_deer_pres + (1 | Location) + (1 | trapdays)	**20**	0.03–0.08	0.00–1.95
Chamois (250 m)	Chamois_pres ∼ elevation_z + julian_day_z + min_temp_z + precip24h_log_z + Red_deer_pres + (julian_day_z:Red_deer_pres) + max_temp_z + eastness_z + northness_z + habitat_type + Roe_deer_pres + slope_z + (1 | Location) + (1 | trapdays)	**7**	0.10–0.28	0.00–1.99
Roe deer (1 km)	Roe_pres ∼ habitat_type + elevation_z + julian_day_z + min_temp_z + max_temp_z + eastness_z + northness_z + slope_z + precip24h_log_z + Red_deer_pres + Chamois_pres + (1 | Location) + (1 | trapdays)	**32**	0.02–0.06	0.00–1.99

Continued on next page

Model	Model (averaged; formula incl. random effects)	Top	Weight	ΔAICc
Roe deer (250 m)	Roe_pres ~ habitat_type + elevation_z + julian_day_z + min_temp_z + max_temp_z + eastness_z + northness_z + slope_z + precip24h_log_z + Red_deer_pres + Chamois_pres + (1 | Location) + (1 | trapdays)	**9**	0.08–0.21	0.00–1.99
Red deer (1 km)	Red_deer_pres ~ Chamois_pres + habitat_type + elevation_z + julian_day_z + Roe_pres + eastness_z + northness_z + slope_z + max_temp_z + precip24h_log_z + (1 | Location) + (1 | trapdays)	**9**	0.07–0.20	0.00–1.99
Red deer (250 m)	Red_deer_pres ~ Chamois_pres + habitat_type + elevation_z + julian_day_z + min_temp_z + precip24h_log_z + Roe_pres + (Chamois_pres:julian_day_z) + max_temp_z + slope_z + eastness_z + northness_z + (1 | Location) + (1 | trapdays)	**11**	0.06–0.15	0.00–1.98

3.1.1 Roe deer

For roe deer, the model-averaged estimates showed consistent correlations with several environmental factors, which, however, varied across spatial resolution.

1 km grid

Based on summed Akaike weights (w^+), elevation (m) had the highest relative importance ($w^+_{\text{elev}} = 1.00$) and was included in all Top models. The next most frequent predictor was minimum temperature ($w^+_{\text{minTemp}} = 0.67$).

Elevation was the only significant covariate included in each of the Top models on the 1km grid (Figure 3.1a). The presence of red deer and chamois had a marginal or very uncertain effect on the presence of roe deer (Figure 3.1a). Roe deer presence decreased with increasing elevation on the 1 km grid ($\beta = -1.87,\ 95\%\,\text{CI} = [-2.75, -1.01]$; Figure 3.1b).

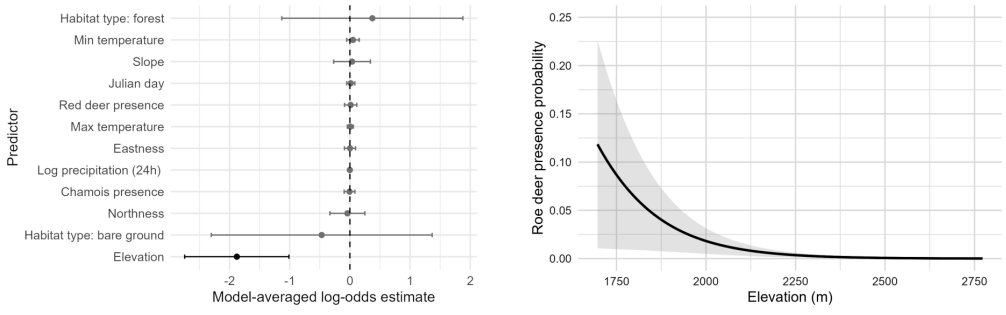

(a) **(b)**

Figure 3.1: Model-averaged results for roe deer presence on the 1 km grid: (a) Forest plot of fixed-effect coefficients with 95% CI (black = significant, grey = non-significant); (b) Effect of elevation on presence probability: Line shows marginal model-averaged predictions of roe deer presence probability from binomial GLMMs (logit link; focal covariate varied, all other predictors at reference values: factors at reference level, z-standardised covariates at 0; back-transformed from the linear predictor to the probability scale using the inverse logit). Shaded bands indicate ±1 SE on the probability scale (Delta-method approximation).

250 m grid

On the 250 m grid, elevation, habitat type, Julian day and red deer presence all showed a maximum importance of $w^+ = 1.00$ and were included in each of the subset models (Figure 3.2).

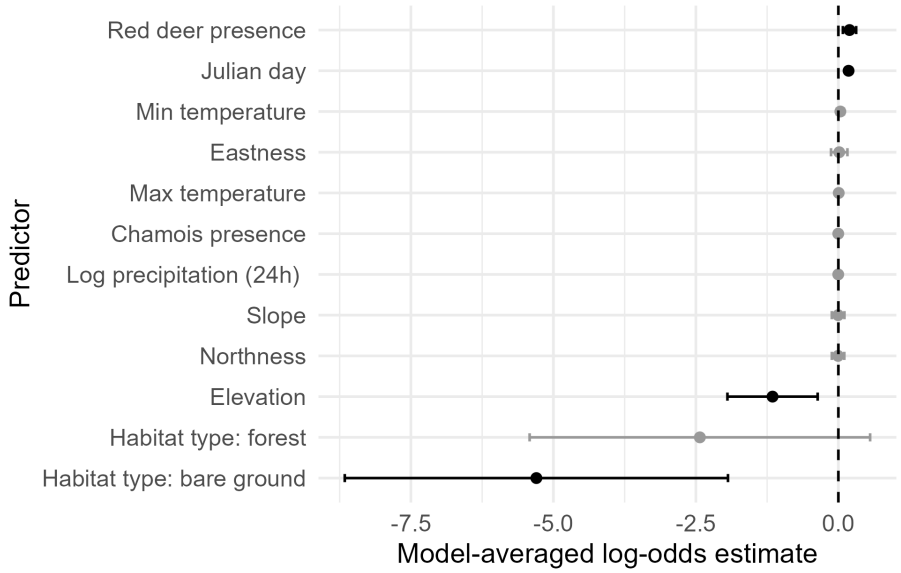

Figure 3.2: Forest plot showing the model-averaged coefficients and 95% CI for predictors in the roe deer model at 250 m resolution. Significant effects are shown in black, non-significant in grey.

With increasing elevation, roe deer presence probability decreased ($\beta = -1.155$, 95% CI $= [-1.947, -0.363]$; Figure 3.3a), and in the later study period, with increasing Julian day, increased significantly ($\beta = 0.179$, 95% CI $= [0.125, 0.234]$, Figure , 3.3b).

There was a positive correlation between the presence of red deer and the probability of roe deer occurence on the 250 m grid. The latter increased with the presence of red deer within 24 hours at a location ($\beta = 0.196$, 95% CI $= [0.079, 0.312]$, Figure 3.3c). The habitat type bare ground showed a significant negative effect compared to the reference habitat type, meadow ($\beta = -5.299$, 95% CI $= [-8.661, -1.937]$, Figure 3.3d). The remaining covariates for weather, slope, northness, eastness and chamois presence showed no significant effects on roe deer presence probability and were not included in many of the Top Models (Appendix C).

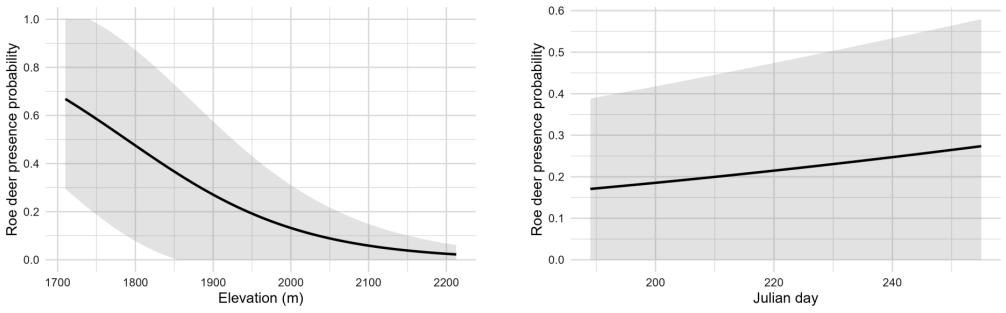

(a) **(b)**

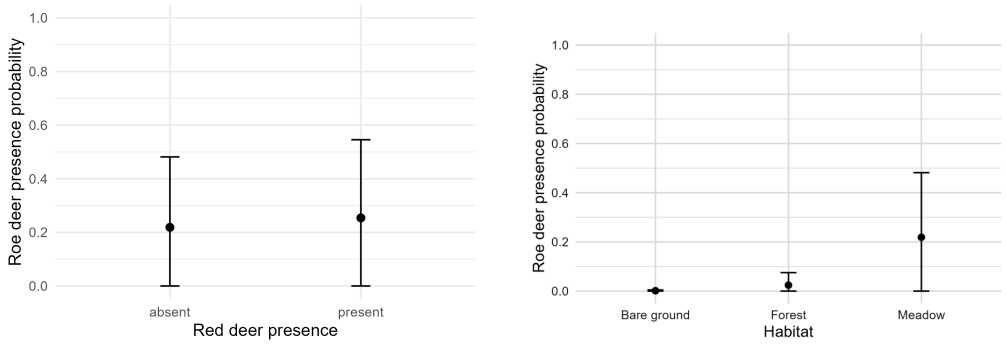

(c) **(d)**

Figure 3.3: Model-averaged results for roe deer presence on the 250 m grid: (a) Elevation, (b) Julian day, (c) Red deer presence, (d) Habitat type (bare ground significant). Lines or points show marginal model-averaged predictions of roe deer presence probability from binomial GLMMs (logit link; focal covariate varied, all other predictors at reference values: factors at reference level, z-standardised covariates at 0; back-transformed from the linear predictor to the probability scale using the inverse logit). Shaded bands or whiskers indicate ± 1 SE on the probability scale (Delta-method approximation).

Compared to modelling with red deer presence, the use of red deer count data in the roe deer model at 250 m resulted in an almost identical model structure and results. With the inclusion of red deer counts, the structure of the explanatory effects remained the same: habitat type bare ground and elevation still had the most frequent and robust negative effect, and Julian day had a positive effect on roe deer presence probability. However, with a 95% CI that included 0 and moderate model summed weight ($w^+ > 0.4$), red deer counts became one of the the less robust effects.

With those results on the 250 m, as well as on the 1 km grid Hypothesis H1 is rejected. No spatial segregation between red and roe deer presence was detected at 24 h intervals on the camera trap data. Conversely, there was a positive effect of red deer presence on roe deer presence probability on the 250 m grid.

3.1.2 Chamois

The model results for chamois showed robust directionally stable estimates regardless of spatial resolution.

1 km grid

An interaction between precipitation and the presence of red deer showed a significant improvement in model fit and was included in the global model of the 1 km grid. In addition to elevation and Julian day, this interaction also had a significant effect on chamois presence in the averaged model (Figure 3.4a, 3.4b). The model included the interaction between precipitation and red deer presence (24 h Precipitation × Red_pres), which had a robust positive effect ($\beta = 0.15,\ 95\%\,\mathrm{CI} = [0.035, 0.270]$, $w^+_{\mathrm{int}} = 1.00$). The negative effect of precipitation was mitigated by red deer presence or vice versa (Figure 3.4b).

Elevation showed a robust positive effect ($\beta = 0.35,\ 95\%\,\mathrm{CI} = [0.123, 0.562]$) and was included in 100% of the models ($w^+_{\mathrm{ele}} = 1.00$). With increasing elevation the probability of chamois presence increased (Figure 3.4c). Julian day had a significant negative effect ($\beta = -0.26,\ 95\%\,\mathrm{CI} = [-0.301, -0.213]$), and was also included in

all Top models ($w^{+}_{\text{jul}} = 1.00$). Chamois presence on the 1 km grid decreased over the course of the season (Figure 3.4d).

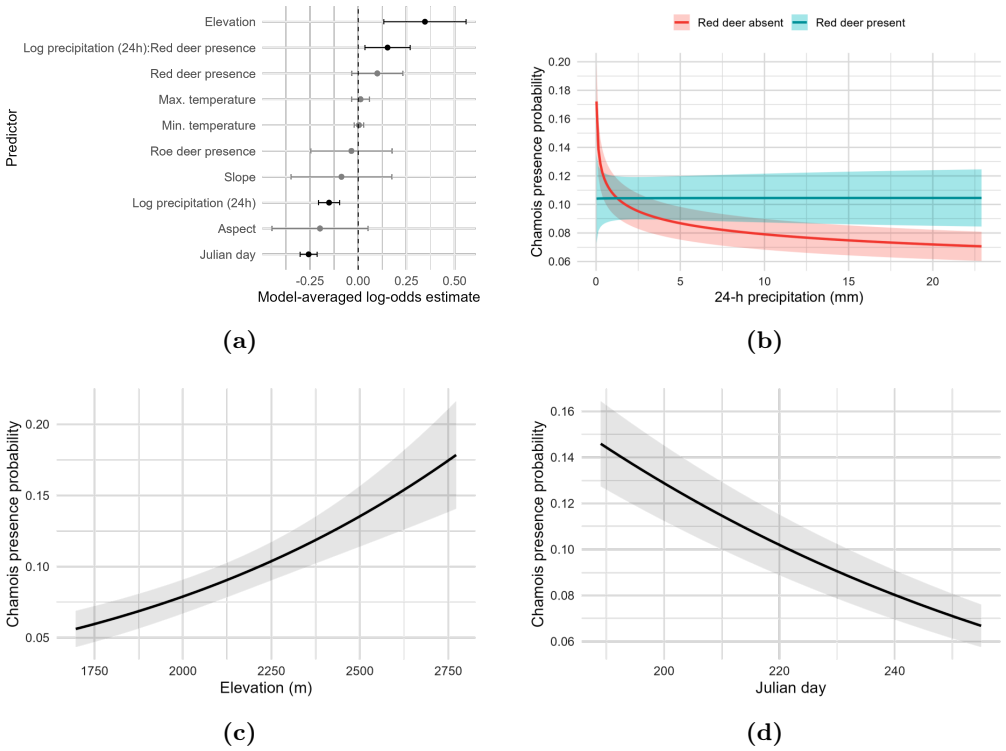

Figure 3.4: Model-averaged results for chamois presence on the 1 km grid: (a) Forest plot with model-averaged coefficients and 95% CI (black = significant, grey = non-significant), (b) Interaction between precipitation and red deer presence, (c) Elevation effect, and (d) Julian day effect. Lines show marginal model-averaged predictions of chamois presence probability from binomial GLMMs (logit link; focal covariate varied, all other predictors at reference values: factors at reference level, z-standardised covariates at 0; back-transformed from the linear predictor to the probability scale using the inverse logit). Shaded bands indicate ±1 SE on the probability scale (Delta-method approximation).

When red deer counts were included instead of presence/absence of red deer the main effects of the model remained robust and `DHARMa` checks indicated no numerical problem. The positive effect of elevation and negative effects of Julian day and precipitation remained unchanged. The effect of red deer counts was included in $w^{+} = 0.72$ of the models, but was not significant.

250 m grid

On the 250 m grid, an interaction between Julian day and red deer presence improved the AICc compared to the global model without interactions and was therefore included. The remaining estimates were similar to those on the 1 km grid.

Based on the summed Akaike weights with $w^{+} = 1.00$, the following key factors influencing the presence of chamois on the 250 m grid were identified (Figure 3.5): a strong positive effect of elevation ($\beta = 0.86$, 95% CI = [0.354, 1.372], Figure 3.6a), and a significant negative effect of the minimum temperature ($\beta = -0.063$, 95% CI = [−0.110, −0.016]), Figure 3.6b). In addition, there was a significant negative effect of precipitation ($\beta = -0.09$, 95% CI = [−0.140, −0.039]), Figure 3.6c). The interaction of Julian day and Red deer presence had a positive effect on chamois presence probability

($\beta = 0.211$, 95% CI $= [0.116, 0.306]$), i.e. the effect of Julian day was enhanced by the presence of red deer or vice versa (Figure 3.6d).

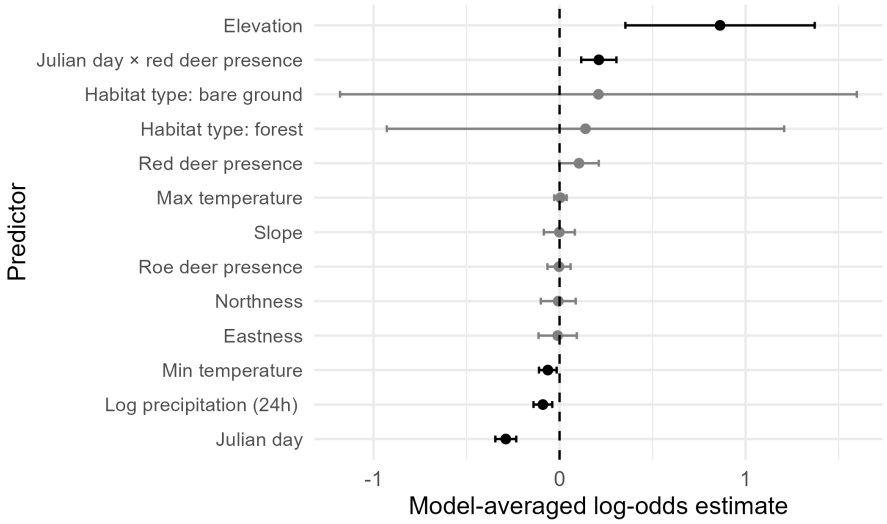

Figure 3.5: Forest plot showing the model-averaged coefficients and 95% CI for predictors in the chamois model at 250 m resolution. Significant effects are shown in black, non-significant in grey.

Northness and eastness, maximum temperature, habitat type, roe deer presence and slope showed no consistent influence (all ($w^+ > 0.2$)), with 95% CI that include zero). The group size of red deer also showed no significant influence on chamois presence at a resolution of 250 m.

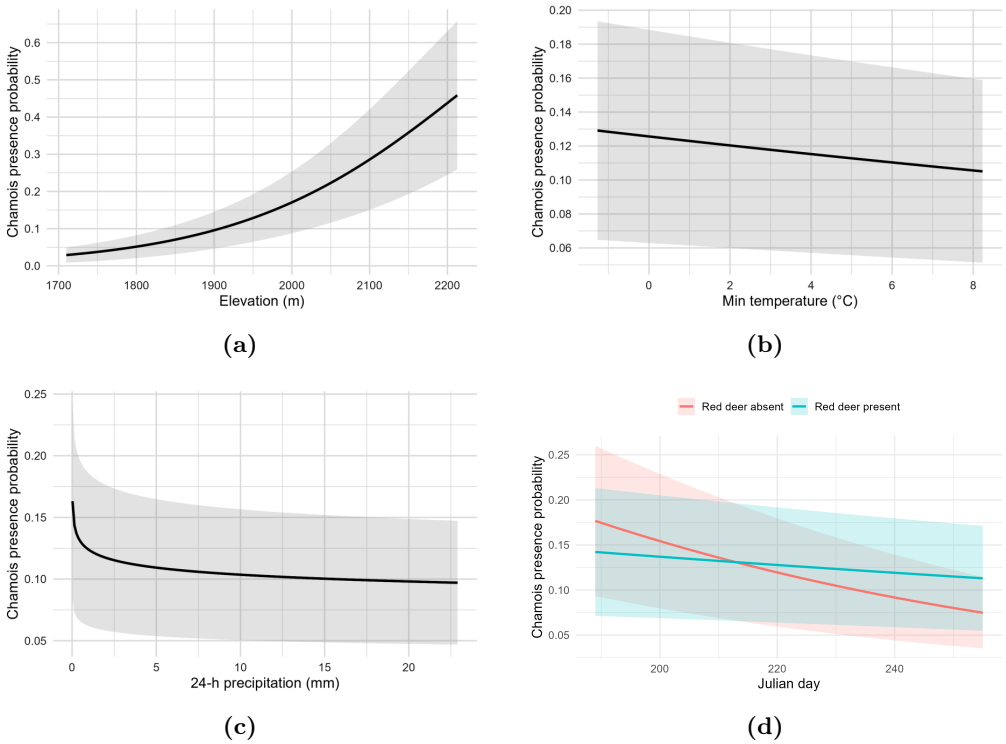

Figure 3.6: Model-averaged results for chamois presence on the 250 m grid: (a) Elevation, (b) Minimum temperature, (c) Precipitation, and (d) Interaction between Julian day and red deer presence. Lines show marginal model-averaged predictions of chamois presence probability from binomial GLMMs (logit link; focal covariate varied, all other predictors at reference values: factors at reference level, z-standardised covariates at 0; back-transformed from the linear predictor to the probability scale using the inverse logit). Shaded bands indicate ±1 SE on the probability scale (Delta-method approximation).

Overall, Hypothesis H3 must be rejected. No negative effect of red deer presence on chamois presence probability was found on either grid.

3.1.3 Red deer

For red deer, model-averaged estimates showed correlations with various environmental variables, but these differed in terms of the direction of the effect or the strength between the grids.

1 km grid

Based on the averaging of 9 models with ΔAICc < 2.0, elevation ($\beta = -0.994$, 95% CI = [−1.56, −0.43], Figure 3.7b), Julian day ($\beta = 0.10$, 95% CI = [0.057, 0.143], Figure 3.7c) and the habitat type bare ground (vs. meadow; $\beta = -2.23$, 95% CI = [−3.57, −0.881], Figure 3.7d) had a significant effect on red deer presence on the 1 km grid. With a relative importance of $w^{+}_{\text{ele}} = 0.81$, the presence of chamois was included in some Top models, but the effect was not significant as the 95% CI exceeds 0 (Figure 3.7a). On the 1 km grid, red deer presence probability increased later in the study period, on meadows and at lower elevations.

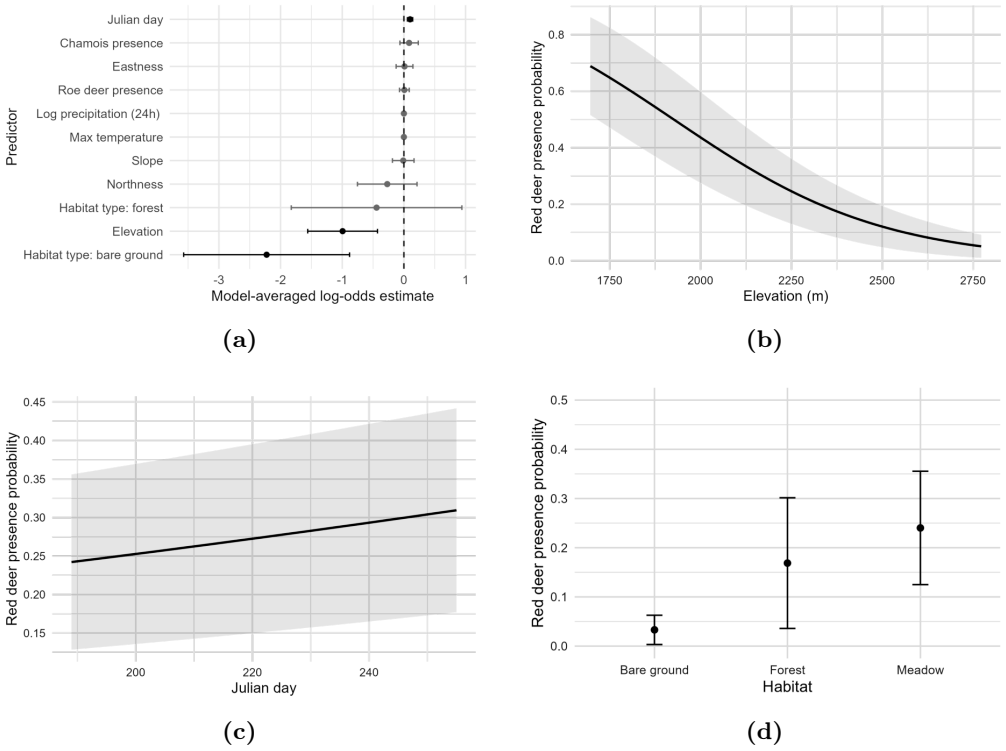

Figure 3.7: Model-averaged results for red deer presence on the 1 km grid: (a) Forest plot showing the model-averaged coefficients and 95% CI (black = significant, grey = non-significant); (b) Elevation effect; (c) Julian day effect; and (d) Habitat type effect (bare ground significant). Lines or points show marginal model-averaged predictions of red deer presence probability from binomial GLMMs (logit link; focal covariate varied, all other predictors at reference values: factors at reference level, z-standardised covariates at 0; back-transformed from the linear predictor to the probability scale using the inverse logit). Shaded bands or whiskers indicate ±1 SE on the probability scale (Delta-method approximation).

250 m grid

On the 250 m grid, elevation showed a significant positive effect on red deer presence probability ($\beta = 0.626$, 95% CI: [0.063, 1.188], Figure 3.8b), whereas the corresponding coefficient was negative in the 1 km model. In addition to the significant negative effect of the habitat type bare ground ($\beta = -4.21$, 95% CI: [−6.797, −1.637], Figure 3.8e), there was a significant negative effect of the habitat type forest on the 250 m grid ($\beta = -3.104$, 95% CI: [−5.435, −0.773], Figure 3.8e). Red deer presence on the 250 m grid was therefore highest on meadows, later during the study period, and with increasing elevation. The presence of roe deer had a significant, slightly positive effect on the presence of red deer ($\beta = 0.189$, 95% CI: [0.073, 0.306], Figure 3.8f), and minimum temperature had a significant, slightly negative effect ($\beta = -0.078$, 95% CI: [−0.115, −0.041], Figure 3.8c). The interaction between Julian day and chamois presence probability had a significant positive effect on red deer presence probability ($\beta = 0.105$, 95% CI: [0.009, 0.200]). The positive effect was enhanced by chamois presence or vice versa (Figure 3.8d).

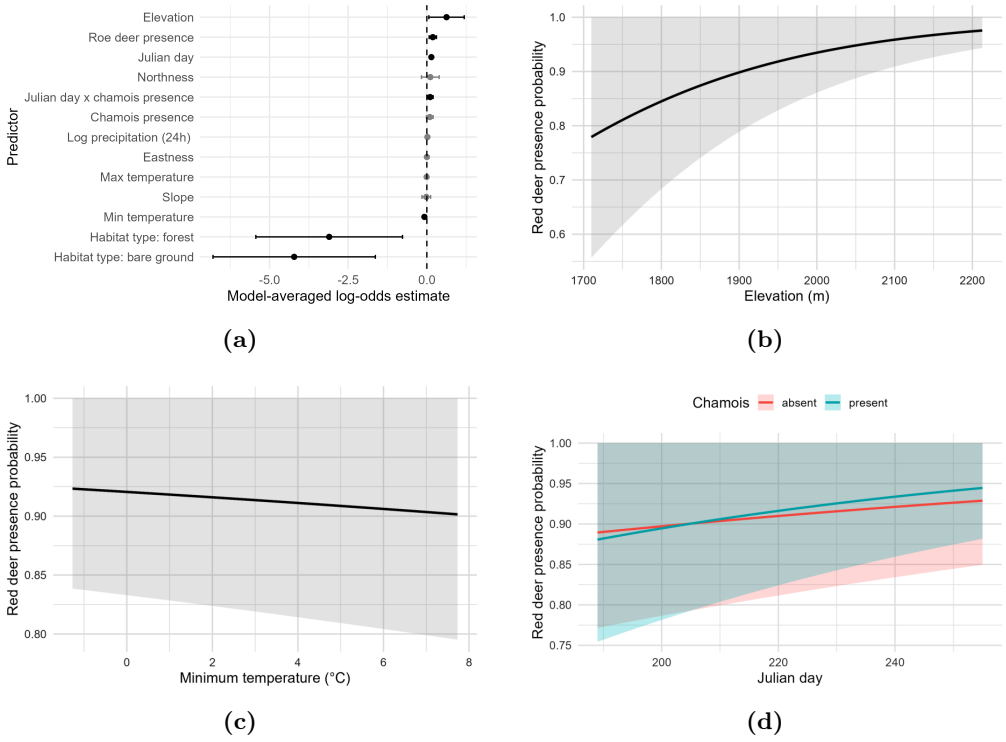

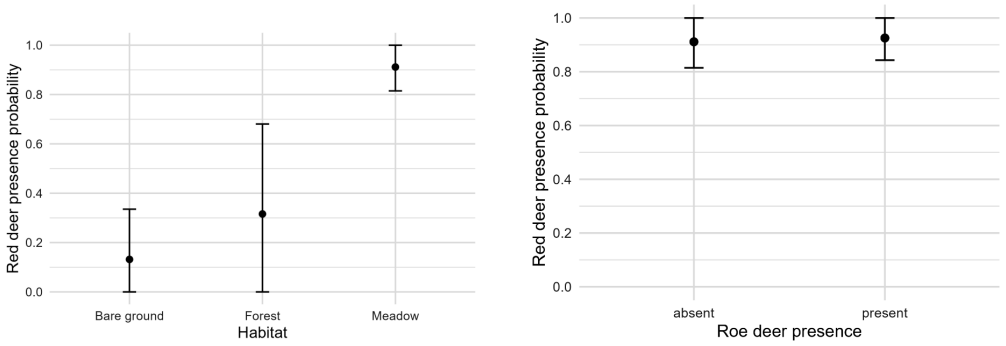

(e) **(f)**

Figure 3.8: Model-averaged results for red deer presence on the 250 m grid: (a) Forest plot showing model-averaged coefficients and 95% CI (black = significant, grey = non-significant), (b) Elevation, (c) Minimum temperature, (d) Interaction between Julian day and chamois presence, (e) Habitat type, and (f) Roe deer presence. Lines or points show marginal model-averaged predictions of red deer presence probability from binomial GLMMs (logit link; focal covariate varied, all other predictors at reference values: factors at reference level, z-standardised covariates at 0; back-transformed from the linear predictor to the probability scale using the inverse logit). Shaded bands or whiskers indicate ±1 SE on the probability scale (Delta-method approximation).

3.2 Temporal analysis

In order to investigate possible temporal interactions between the three species, the intervals per species pair and species direction were modelled, resulting in five averaged models shown in Table 3.2. All included Top models per averaged model can be seen in Appendix C. The temporal intervals models for each species pair showed no anomalies in the visual `DHARMa` diagnostics except for the one that was dropped (chamois ↔ red deer 250 m grid). The sample size of detected temporal intervals was smaller on the 1 km grid than on the 250 m grid. This difference was most pronounced for chamois–roe deer and red deer–roe deer pairs, while the longest intervals were found between chamois and roe deer on the 1 km grid (Table 3.3). In all models, the response variable represents temporal intervals between detections. In the effect plots (Figures 3.9b - 3.14f), the y-axis is labelled "predicted mean distance (min)", which in this context refers to the predicted mean temporal interval between detections (i.e. distance in time (minutes)).

Table 3.2: Model-averaged temporal GLMMs. Formulas show the fixed effects across the respective Top models; all models include random intercepts for `Location` and `Year`. Weight and ΔAICc ranges refer to the models included (Top) in the corresponding Top-model set.

Model	Model (averaged; formula incl. random effects)	Top	Weight	ΔAICc
Roe deer—Red deer (1 km)	*min_intervals* ~ species pair + habitat_type + elevation_z + Julian_day_z + slope_z + precip_1h_z + time_cos + air_temp_2m_z + (1 | LocationNumber) + (1 | Year) *disp* ~ habitat_type + elevation_z + Julian_day_z + 1	**21**	0.03–0.09	0.00–1.99

Continued on next page

Model	Model (averaged; formula incl. random effects)	Top	Weight	ΔAICc
Roe deer—Red deer (250 m)	*min_intervals* ~ species pair + habitat_type + elevation_z + Julian_day_z + slope_z + precip_1h_z + time_cos + time_sin + air_temp_2m_z + (1 | LocationNumber) + (1 | Year) *disp* ~ habitat_type + elevation_z + 1	**10**	0.07–0.18	0.00–1.75
Roe deer—Chamois (1 km)	*min_intervals* ~ species pair + habitat_type + elevation_z + Julian_day_z + slope_z + precip_1h_z + time_cos + time_sin + air_temp_2m_z + (1 | LocationNumber) + (1 | Year) *disp* ~ habitat_type + 1	**11**	0.06–0.16	0.00–1.99
Roe deer—Chamois (250 m)	*min_intervals* ~ species pair + elevation_z + Julian_day_z + slope_z + precip_1h_z + time_cos + time_sin + air_temp_2m_z + (1 | LocationNumber) + (1 | Year) *disp* ~ elevation_z + Julian_day_z + 1	**11**	0.06–0.16	0.00–1.92
Chamois—Red deer (1 km)	*min_intervals* ~ species pair + habitat_type + elevation_z + Julian_day_z + precip_1h_z + time_cos + time_sin + air_temp_2m_z + (1 | LocationNumber) + (1 | Year) *disp* ~ elevation_z + Julian_day_z + 1	**4**	0.17–0.45	0.00–2.00

Table 3.3: Summary of pairwise intervals per species pair at both spatial resolutions (250 m and 1 km grids).

Grid	Species pair	n	Locations	Years	Median (min)	Q25	Q75
250 m	Red → Red	9713	71	4	1018	201	2651
250 m	Red → Chamois	8310	71	4	7371	2106	20943
250 m	Red → Roe	6867	62	4	5261	1789	13064
250 m	Chamois → Chamois	3739	73	4	1414	215	4537
250 m	Chamois → Red	3463	71	4	1893	771	4661
250 m	Roe → Red	2294	62	4	1698	701	4136
250 m	Roe → Roe	2158	59	4	2368	563	6367
250 m	Roe → Chamois	2012	60	4	12536	4142	31072
250 m	Chamois → Roe	1658	60	4	8077	2807	20378
1 km	Red → Red	5762	58	4	909	101	2761
1 km	Red → Chamois	5123	61	4	6845	2402	18526
1 km	Chamois → Chamois	4552	72	4	1186	61	4324
1 km	Chamois → Red	2655	57	4	4662	1470	13808
1 km	Red → Roe	2473	32	4	10372	3620	25116
1 km	Roe → Red	734	29	4	2238	867	5092
1 km	Roe → Roe	702	25	4	2102	556	6224
1 km	Roe → Chamois	590	31	4	13628	4174	28959
1 km	Chamois → Roe	575	31	4	12340	4258	28083

3.2.1 Roe deer - red deer temporal interaction

1 km grid

Model averaging for temporal intervals between roe deer ↔ red deer events on the 1 km grid based on $\Delta\text{AICc} \leq 2$ yielded $n = 21$ models with similar weight distributions in the Top set. Significant positive effects were found for Julian day ($\beta = 0.401$, 95% CI = [0.361, 0.441], Figure 3.9b) and temperature ($\beta = 0.063$, 95% CI = [0.026, 0.099], Figure 3.9c). Intervals between events became longer later in the season and with increasing temperature. The

only significant negative effect was shown by the species pair direction roe deer → red deer ($\beta = -0.768$, 95% CI = [−0.886, −0.649], Figure 3.9d). Intervals between a roe deer and red deer event were significantly shorter than those between a red deer and subsequent roe deer event. Other environmental and location variables had no significant effect on the temporal intervals between events (Figure 3.9a).

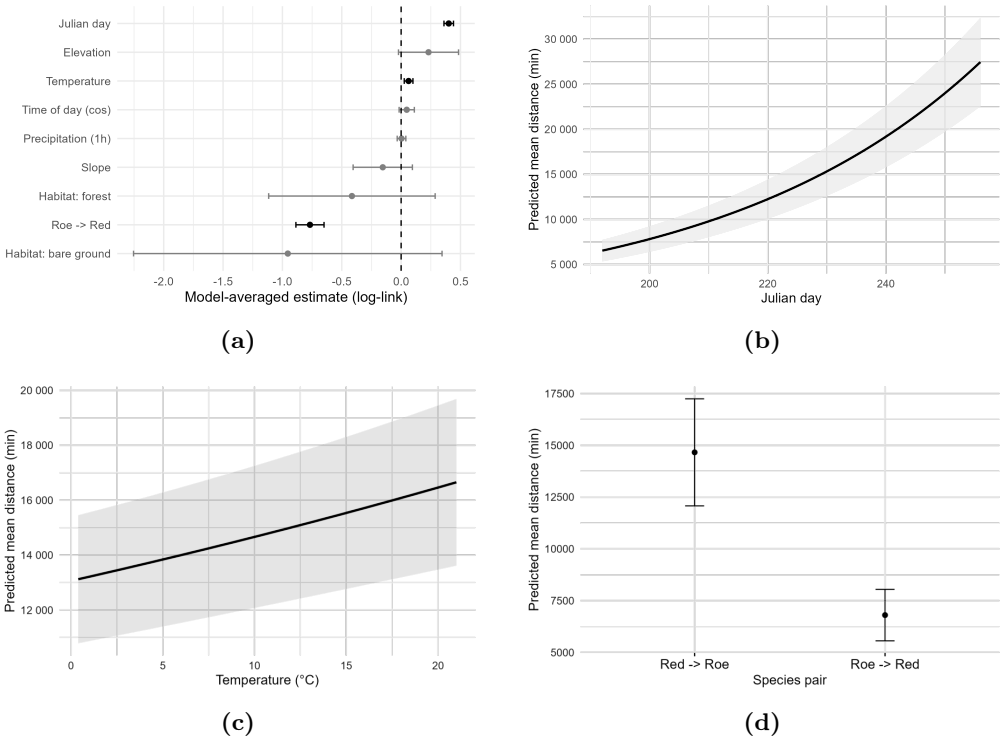

Figure 3.9: Model-averaged results for temporal intervals between roe deer and red deer on the 1 km grid: (a) Forest plot showing model-averaged coefficients and 95% CI (black = significant, grey = non-significant), (b) Julian day effect, (c) Temperature effect, and (d) Species pair effect. Lines or points show marginal model-averaged predictions of temporal intervals from Gamma GLMMs (log link; focal covariate varied, all other predictors at reference values: factors at reference level, z-standardised covariates at 0; back-transformed from the linear predictor to the original scale using the inverse log). Shaded bands or whiskers indicate ±1 SE on the original scale (Delta-method approximation).

250 m grid

Julian day ($\beta = 0.104$, 95% CI = [0.0787, 0.130], Figure 3.11a) and temperature ($\beta = 0.075$, 95% CI = [0.039, 0.111], Figure 3.11b) also had a significant positive effect on the temporal intervals on the 250 m grid (Figure 3.10). The species direction roe deer → red deer again had a significant negative effect ($\beta = -0.83$, 95% CI = [−0.891, −0.769], Figure 3.11c).

In addition to environmental and species influences, there was a diurnal pattern of intervals, which was mainly influenced by the sine component ($\beta = 0.056$, 95% CI = [0.019, 0.100], 3.11d) but not by the cosine variable ($\beta = 0.0321$, 95% CI = [−0.011, 0.075]).

Overall the intervals between roe deer and red deer increased over the course of the study period and as the maximum daily temperature rose. In addition, the intervals changed over the course of the day (Figure 3.11d).

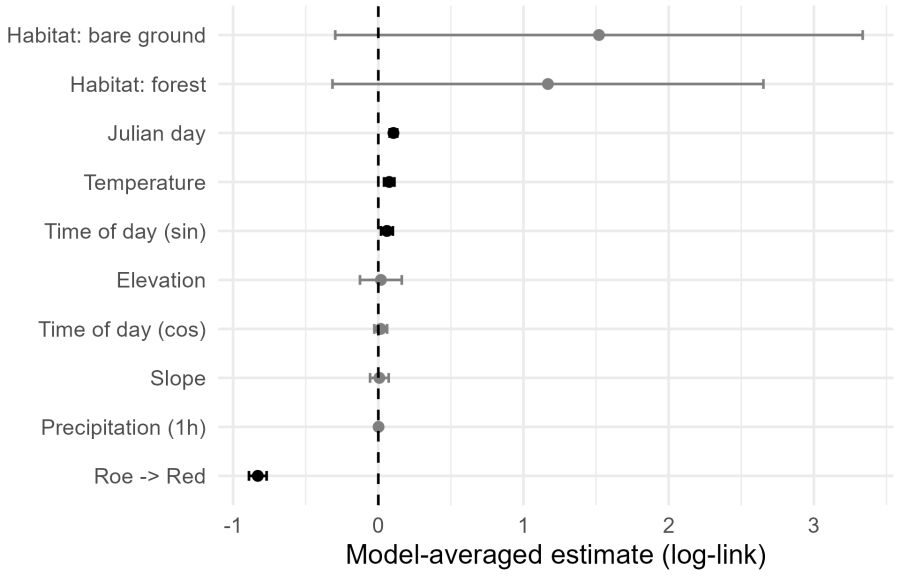

Figure 3.10: Forest plot showing the model-averaged coefficients and 95% CI for predictors in the temporal intervals model between roe deer and red deer at 250 m resolution. Significant effects are shown in black, non-significant in grey.

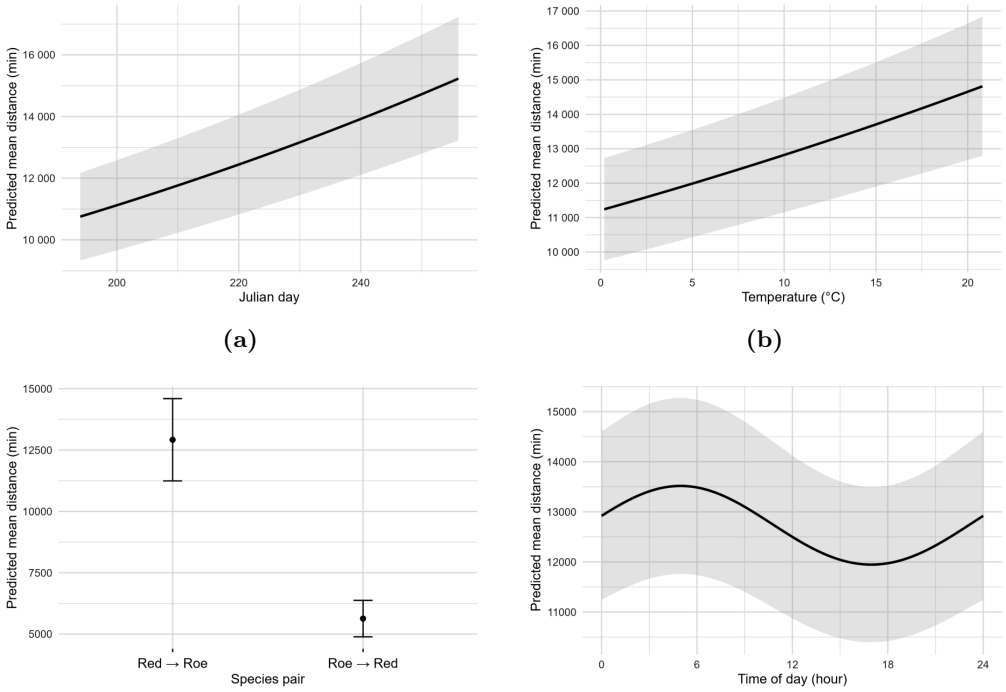

Figure 3.11: Model-averaged results for temporal intervals between roe deer and red deer on the 250 m grid: (a) Julian day, (b) Temperature, (c) Species pair, (d) Time of day. Lines or points show marginal model-averaged predictions of temporal intervals from Gamma GLMMs (log link; focal covariate varied, all other predictors at reference values: factors at reference level, z-standardised covariates at 0; back-transformed from the linear predictor to the original scale using the inverse log). Shaded bands or whiskers indicate ±1 SE on the original scale (Delta-method approximation).

Contrary to Hypothesis H2 derived from the literature, a temporal displacement of roe deer by red deer could be detected. Both on the 250 m grid and on the 1 km grid, roe deer took longer to appear after a red deer event than vice versa.

3.2.2 Roe deer - chamois temporal interactions

1 km grid

At 1 km resolution, the temporal intervals between chamois and roe deer events were associated with seasonal timing, temperature, and habitat (Figure 3.12a). Intervals between events increased with Julian day ($\beta = 0.609$, 95% CI = [0.545, 0.672], Figure 3.12b) and temperature ($\beta = 0.062$, 95% CI = [0.002, 0.123], Figure 3.12c). The habitat type forest showed a significantly negative effect compared to the reference habitat type meadow ($\beta = -0.627$, 95% CI = [−1.134, −0.119], Figure 3.12d).

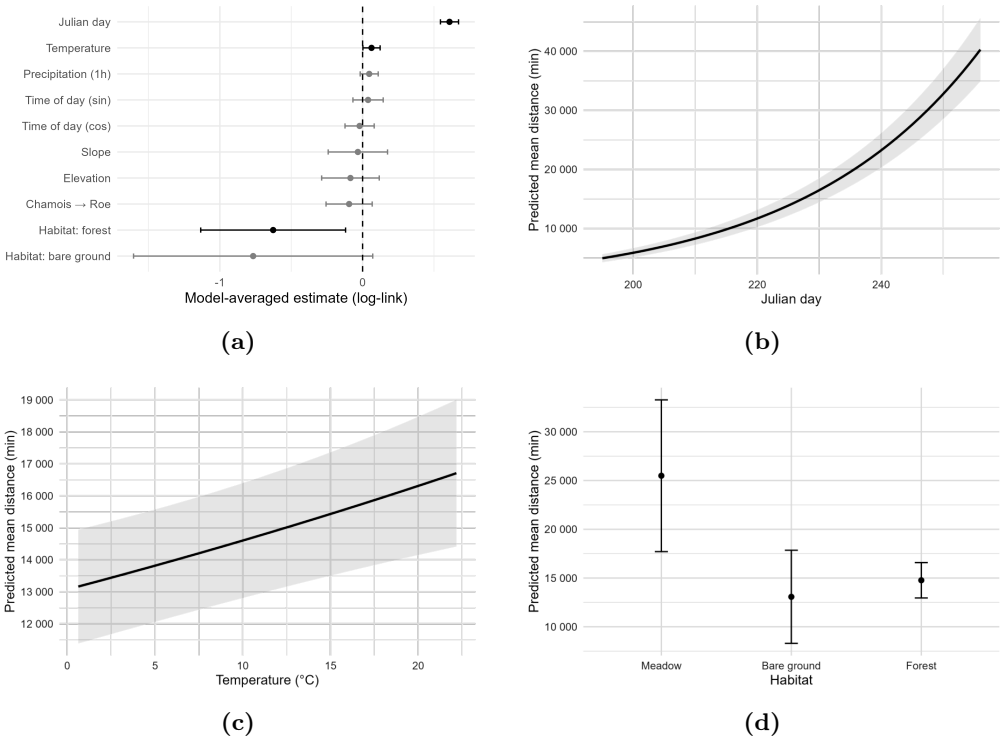

Figure 3.12: Model-averaged results for temporal intervals between roe deer and chamois on the 1 km grid: (a) Forest plot showing model-averaged coefficients and 95% CI (black = significant, grey = non-significant), (b) Julian day effect, (c) Temperature effect, and (d) Habitat type effect (forest significant). Lines or points show marginal model-averaged predictions of temporal interval from Gamma GLMMs (log link; focal covariate varied, all other predictors at reference values: factors at reference level, z-standardised covariates at 0; back-transformed from the linear predictor to the original scale using the inverse log). Shaded bands or whiskers indicate ±1 SE on the original scale (Delta-method approximation).

250 m grid

At 250 m resolution, the chamois–roe deer model identified Julian day, temperature, and species-pair direction as supported predictors, whereas Habitat type did not enter the averaged set (Figure 3.13a). As on the 1 km grid, Julian day ($\beta = 0.433$, 95% CI = [0.3778, 0.477], Figure 3.13b) and temperature ($\beta = 0.095$, 95% CI = [0.044, 0.146], Figure 3.13c) both showed a significant effect on the temporal intervals between roe deer and chamois. On the 250 m grid, there was also a significant negative effect of the species pair direction chamois → roe deer compared to the reference direction roe deer → chamois ($\beta = -0.183$, 95% CI = [−0.287, −0.079], Figure 3.13d). On average, it took longer for a chamois to appear at the same location on the 250 m grid after a roe deer event than vice versa.

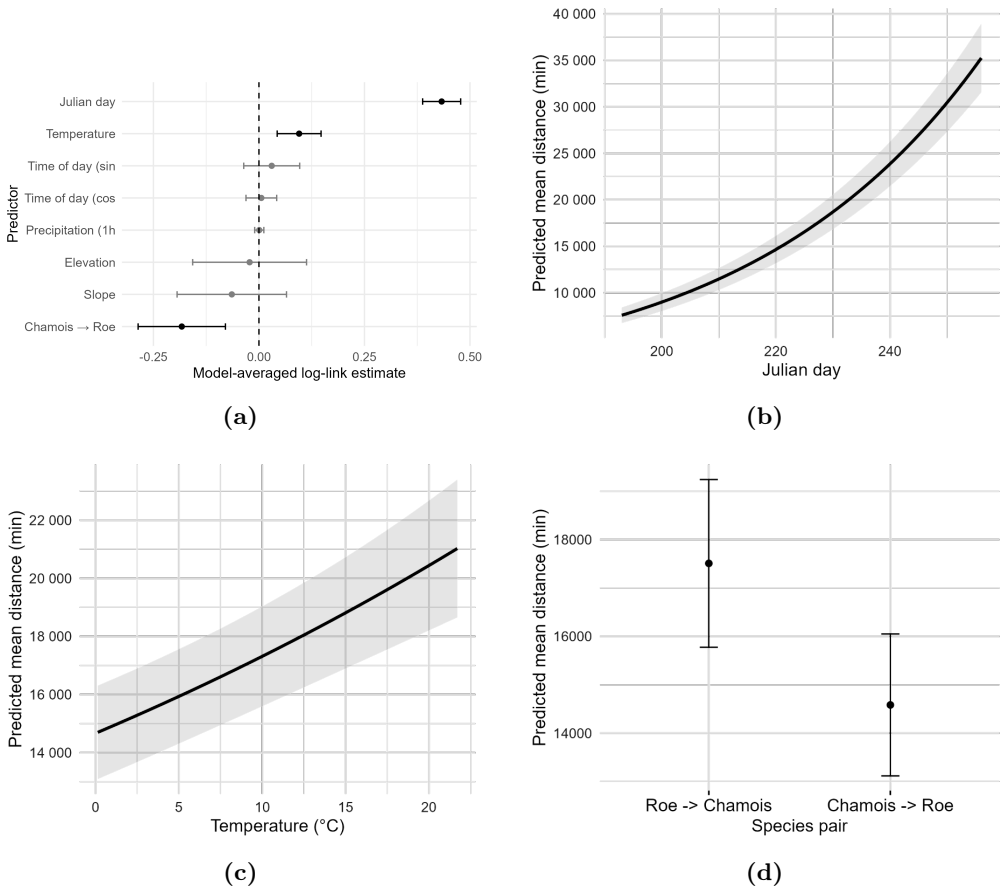

Figure 3.13: Model-averaged results for temporal intervals between roe deer and chamois on the 250 m grid: (a) Forest plot showing model-averaged coefficients and 95% CI (black = significant, grey = non-significant), (b) Julian day effect, (c) Temperature effect, and (d) Species pair effect. Lines or points show marginal model-averaged predictions of temporal intervals from Gamma GLMMs (log link; focal covariate varied, all other predictors at reference values: factors at reference level, z-standardised covariates at 0; back-transformed from the linear predictor to the original scale using the inverse log). Shaded bands or whiskers indicate ±1 SE on the original scale (Delta-method approximation).

3.2.3 Chamois - red deer temporal interaction

For the red deer–chamois pair, inter-event intervals were associated with Julian day, temperature, habitat, diel activity, and species-pair direction (Figure 3.14a). Julian day in particular showed a significant, strongly positive effect on intervals between red deer and chamois events ($\beta = 0.545$, 95% CI = [0.517, 0.572], Figure 3.14b). Temperature ($\beta = 0.053$, 95% CI = [0.017, 0.090], Figure 3.14c) and habitat type bare ground compared to the reference habitat type meadow ($\beta = 0.547$, 95% CI = [0.263, 0.832], Figure 3.14d) also had a significantly positive influence on the intervals. Intervals between red deer and chamois events increased with rising temperature and on bare ground. In addition to the environmental variables, there was also a time-of-day effect on the intervals, which was mainly driven by the significant sine component ($\beta = 0.066$, 95% CI = [0.022, 0.110], Figure 3.14f) and a non-significant cosine component ($\beta = 0.0456$, ; 95% CI = [−0.001, 0.092]). In addition, the species pair direction chamois → red deer showed a significant decrease on interval sizes compared to the reference direction red deer → chamois ($\beta = -0.4409$, 95% CI = [−0.524, −0.374], Figure 3.14e). The intervals between chamois and red deer events were shorter than those between red deer events and the next chamois occurrence at the same location.

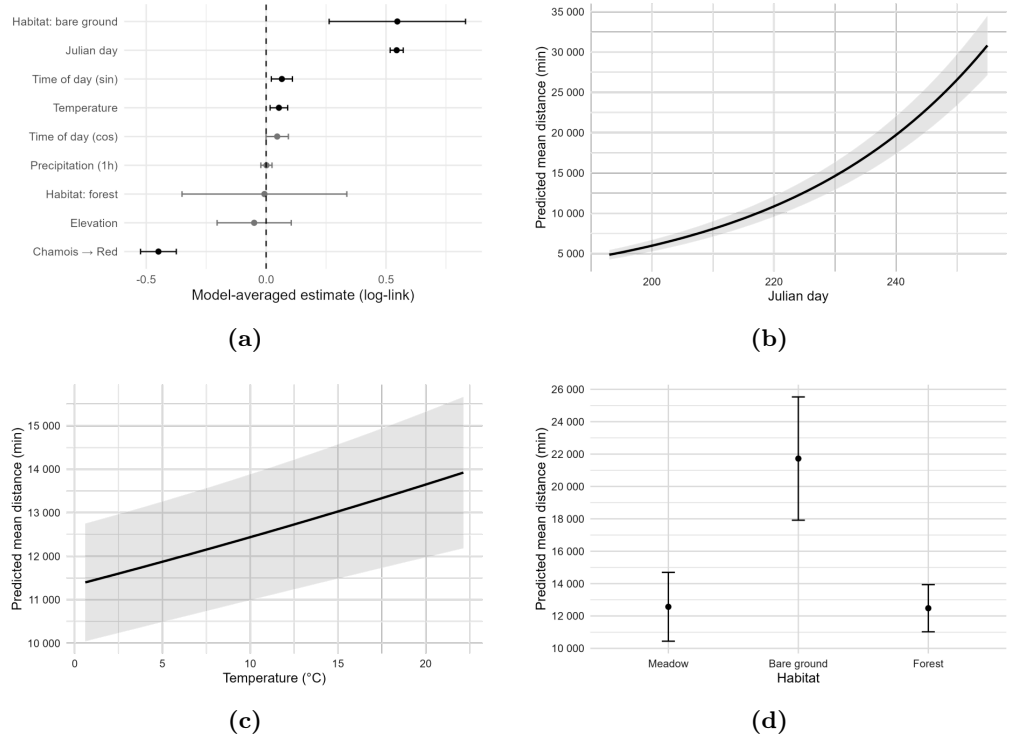

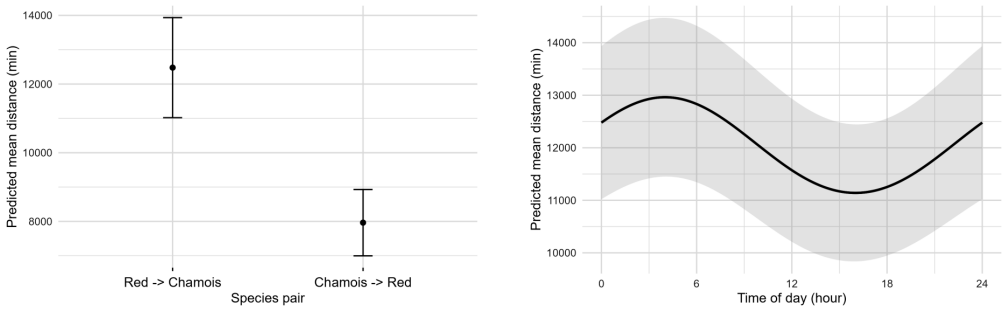

(e) **(f)**

Figure 3.14: Model-averaged results for temporal intervals between chamois and red deer on the 1 km grid: (a) Forest plot with model-averaged coefficients and 95% CI (black = significant, grey = non-significant), (b) Julian day, (c) Temperature, (d) Habitat type (bare ground significant), (e) Species pair, and (f) Time of day. Lines or points show marginal model-averaged predictions of temporal intervals from Gamma GLMMs (log link; focal covariate varied, all other predictors at reference values: factors at reference level, z-standardised covariates at 0; back-transformed from the linear predictor to the original scale using the inverse log). Shaded bands or whiskers indicate ±1 SE on the original scale (Delta-method approximation).

Hypothesis H4 was confirmed by the results shown on the 1 km grid. There is a one-sided interval difference between chamois and red deer, indicating one sided temporal segregation.

Chapter 4

Discussion

4.1 Key findings and context

The aim of this study was to investigate spatial and temporal interactions between roe deer, chamois and red deer based on camera trap data. The focus was on possible displacement of roe deer and chamois by red deer, to find out whether avoidance mechanisms occur in the study area. In the spatial analysis, the main factors influencing the presence of the three species were elevation, seasonality and, in some models, habitat type. No evidence of displacement was found between species.

However, the temporal analysis revealed that roe deer and chamois kept greater intervals from red deer events than vice versa, which may be an indication of temporal displacement. In the following the spatial and temporal analysis results will be examined and placed in the context of other study results in order to address broader ecological implications.

4.2 Spatial patterns and environmental drivers

The spatial analysis aimed to identify whether there was any spatial partitioning between roe deer, chamois and red deer. The results demonstrated that environmental gradients, rather than interspecific interactions, were the main determinants of species occurrence patterns across both spatial scales.

Elevation, seasonality and habitat were the most important factors for all three species. However, the relative importance and effect strength varied between the 1 km and 250 m grids, showing scale-dependent habitat selection. The scale-dependent effects are particularly noticeable in roe deer and red deer. Elevation was the only significant effect on roe deer presence probability on the 1 km grid, while other significant environmental variables became significant on the 250 m grid. These include additional factors such as seasonality and a preference for meadows over bare ground, which is in line with their use of open areas during favourable conditions and good food quality (Johnson et al., 1995; Storms et al., 2008; Mancinelli, S. et al., 2015). This reflects the finer environmental heterogeneity captured at smaller scales (Cromsigt and Olff, 2006). For red deer, the effect of elevation changed from negative on the 1 km grid to positive on the 250 m grid. This structure suggests that the smaller and therefore more detailed grid captures local habitat heterogeneity and represents finer resource selection patterns that would have remained undetected on a larger scale.

The scale dependence of the effects is also evident in the varying effect strengths of a predictor for the same species. For example, the influence of elevation on the probability of detecting chamois is significantly stronger on the 250 m grid ($\beta = 0.86$) than on the 1 km grid ($\beta = 0.35$). This difference can be explained on the one hand by the different spatial resolution (Jelinski and Wu, 1996; Cromsigt and Olff, 2006). On the finer scale, local relief structures such as forest edges, slope edges or rocky areas are mapped more accurately, while this heterogeneity is averaged out on the 1 km area due to aggregation (Jelinski and Wu, 1996).

The 250 m grid on the other hand, is predominantly located in areas at lower elevations and with denser forest cover. Even small differences in elevation can be associated with transitions to steeper terrain or more open habitat. Those are particularly relevant as microhabitats for chamois (Anderwald et al., 2016; Kavčić et al., 2021). The stronger elevation effect can

therefore be interpreted as an expression of finer habitat selection mechanisms on the 250 m grid, which are attenuated on a larger scale by averaging effects.

Beyond these biological explanations, methodological factors also contribute. It should be noted that all predictors within each grid were z-standardized. Differences in β values therefore reflect both biological scale dependence and differences in the variance of elevation distribution and aggregation effects (Greenland et al., 1986; Jelinski and Wu, 1996). A more detailed methodological discussion can be found in the section on methodological limitations.

In addition to these environmental gradients, weak interspecific interactions were detected that can be linked to the scale dependence of environmental variables. On the 250 m grid, roe deer presence probability was slightly positively correlated with red deer presence, and vice versa. For chamois at the 1 km grid, a slightly reduced negative effect of precipitation appeared when red deer were present. As most previous studies have found either neutral or negative effects of red deer on the spatial distribution of other cervids (Latham et al., 1996; Torres et al., 2012; Ferretti et al., 2019; Anderwald et al., 2016; Borkowski et al., 2021; Donini et al., 2025), this was unexpected. This apparent positive relationship likely reflects shared environmental preferences rather than true facilitation (Blanchet et al., 2020). The marginal positive effect of roe deer on red deer further suggests that both species respond to similar habitat conditions rather than directly influencing each other especially at finer spatial resolution. Roe deer select habitats primarily based on good food quality and variability (Mancinelli, S. et al., 2015), and the distribution of red deer and chamois depends in part on productivity gradients in the respective habitats (Anderwald et al., 2016). In more productive areas, Anderwald et al. (2016) observed negative effects of red deer density on the horn growth of young chamois. No such correlation was found in less productive areas. Such productivity effects, which can influence the spatial distribution of species, were not taken into account in the analysis and may influence the results. This supports common responses to resource gradients (such as higher primary productivity) that can be mistaken for interspecific effects. This interpretation is consistent with the caution expressed by Blanchet et al. (2020) regarding the risk of false species associations in presence–absence models that do not fully account for environmental covariation. Environmental factors that are not taken into account can cause apparent correlations between coexisting species. (Dormann et al., 2018; Blanchet et al., 2020).

For the spatial analysis, it can thus be concluded that the three species inhabit similar habitats in the National Park, with partially differing preferences. Chamois were found at higher elevations and were more likely to be present at the beginning of the season. The probability of red deer and roe deer being present increased later in the study period. Importantly, there was no evidence that red deer presence reduced the probability of roe deer or chamois being present at the same camera location. These results are in line with those of Donini et al. (2025) in the Alps. They also found no effect of red deer abundance on the occupancy probability of roe deer but effects of other environmental variables such as elevation and slope (Donini et al., 2025). In contrast, the results of Torres et al. (2012) and Borkowski et al. (2021) have found a change in the spatial use of roe deer with increased abundance of red deer. The same applied to Alpine chamois (Anderwald et al., 2015; Corlatti et al., 2019; Ferretti et al., 2019). This could indicate that such displacement effects can depend on habitat availability and productivity. In resource-limited alpine landscapes, limited suitable habitat is likely to reduce the possibility of spatial segregation between species (Donini et al., 2025). Due to their generalist lifestyle, red deer are widespread throughout the park in summer (Haller, 2002). In terms of space, roe deer and chamois have little alternative habitat due to their more limited habitat selection and need for high quality, variable food in case of roe deer (Storms et al., 2008; Mancinelli, S. et al., 2015; Anderwald et al., 2015).

The overlap in habitat use thus supports the absence of spatial displacement, but it may increase the potential for temporal segregation as a coexistence mechanism, which is explored in the following section.

4.3 Temporal patterns and environmental drivers

When two species use the same habitat due to identical habitat requirements, temporal partitioning may occur during spatial co-use, which may be an indication that one species

is being displaced (Di Bitetti et al., 2010; Šprem et al., 2015; Kavčić et al., 2021; Marshall et al., 2023). Especially in habitat-limited and heterogeneous areas as the alpine Il Fuorn area (Anderwald et al., 2016) such temporal avoidance can become of importance.

To assess potential temporal avoidance among species pairs in the area, directional time intervals betweens species detections were analysed. The temporal analysis revealed species pair-specific differences in the intervals, which varied over the day and study period. A longer interval between species A to species B than vice versa indicates a possible avoidance or displacement of B by A (Niedballa et al., 2019).

These directional intervals may represent the possible displacement of roe deer and chamois by red deer as postulated in the hypotheses H2 and H4. Similar approaches have been used, for example, by Marshall et al. (2023) and Smith et al. (2023) to detect temporal displacement between carnivores. The directional intervals in this study show greater intervals between red deer and roe deer at both resolutions, between red deer and chamois on the 1 km grid, and between roe deer and chamois on the 250 m grid. An asymmetric temporal distribution in favour of red deer emerged. This indicates that the often superior competitor (red deer) temporarily has priority in shared habitats, while the smaller species (roe deer and chamois) change their timing accordingly.

These trends may be associated with interference at attractive resources (Šprem et al., 2015) and are consistent with the results of Kavčić et al. (2021) who found weak temporal partitioning between roe deer and chamois and the mostly superior competitor red deer due to competition for resources. Even though the spatial analysis found no evidence of displacement, these temporal patterns indicate behavioural segregation on a fine scale. Increasing time intervals towards the end of the study period despite increased presence of roe deer and red deer further emphasises that both species increasingly use the same areas, but at different times. This indicates temporal segregation under intensified competition. Especially at the end of summer and beginning of autumn, sufficient access to high-quality food is essential especially for juveniles (Parker et al., 2009). If exploitative competition occurs during this period, it can lead to fitness losses for the disadvantaged species at the beginning of winter (Parker et al., 2009; Willisch et al., 2013; Anderwald et al., 2024) and thus to a long-term weakening of the respective population. Smith et al. (2023) also found no significant changes in the 24-hour cycles when investigating spatio-temporal relationships between carnivores using comparable methodology, but did find a finer-scale segregation in successive events and less overlap in resource-poor periods due to presumed increased competition (Smith et al., 2023) . Using similar methodology, Marshall et al. (2023) found similar results in carnivores, in which temporal partitioning occurred despite spatial coexistence, and interpreted this as a possible avoidance mechanism for a species, especially where spatial segregation is limited.

However, alternative explanations related to detection probability must also be taken into account. Such directional interval length differences can also be influenced by the detection probability of a species. The greater interval between roe deer and chamois on the 250 m grid could be explained by the fact that the general detection frequency of chamois on the 250 m grid is lower and it takes longer for them to appear (MacKenzie et al., 2002; Sollmann, 2018; Swinkels et al., 2023; Smith et al., 2023; Ferry et al., 2024). Nevertheless, if detection probability were the sole driver, seasonal patterns would be expected to shorten intervals when presence probabilities increase, not the opposite. In contrast, the seasonal changes in intervals align with biological expectations: as the probability of presence of both roe deer and red deer increased over the season, intervals lengthened rather than shortened. This pattern is unlikely under a detection-only explanation. Moreover, the remaining directional patterns are biologically plausible, consistent within each grid, and occur at generally shorter total intervals than for the roe deer–chamois intervals which makes it more plausible to be an interspecies effect. Therefore, different detection frequencies alone do not seem to be the complete explanation for directionally asymmetric intervals between species.

In summary, the spatial analysis showed no strong correlation between the presence of the species, while the results of the temporal analysis indicate behavioural adaptations of the two competitively inferior species.

4.4 Methodological considerations and limitations

The following section deals with methodological considerations that apply specifically to spatial and temporal analyses and discusses general limitations that apply to both approaches.

For the spatial models, several methodological aspects need to be considered when interpreting effect sizes across scales. The model predictors were z-standardised within both spatial resolutions. The regression coefficients therefore reflect a change of one SD per grid. Direct comparisons of the β values between the two grids are therefore only possible to a limited extent, as the SD and the underlying scale variance differ between the grids. In addition, aggregation on a large scale can lead to a weakening of the effects of elevation or other predictors when local heterogeneity is averaged (Greenland et al., 1986; Jelinski and Wu, 1996). Differences in effect (β) sizes were therefore interpreted both biologically (e.g. as fine-scale habitat selection or relief differences) and statistically through different variance structures. The main effects were thus not directly interpreted in terms of their effect strength but in terms of their significance or insignificance.

An exception to this are the significant but very weak effects of roe deer presence, temperature and Julian day on, for example, red deer presence probability on the 250m grid. Model averaging can lead to post-selection bias. Overly complex models are sometimes favoured in AIC analyses, which can lead to a larger number of included predictors and thus to overinterpretation of the importance of predictors (Arnold, 2010; Symonds and Moussalli, 2011). Arnold (2010) suggests reporting all included Top models, as shown in Appendix C, in order to ensure the necessary transparency. Particularly weak effects should therefore be viewed with caution. To mitigate or circumvent this problem, model averaging with the strictest common limit of $\Delta\text{AICc} \leq 2$, rather than selecting one specific model, was used. Averaging is particularly useful when, as in this analysis, no single model stands out in terms of weight (Arnold, 2010; Symonds and Moussalli, 2011). As a further safeguard, according to Arnold (2010), only those effects whose 95% CI do not exceed 0 should be interpreted as significant, which is a more robust approach than using p-values alone. Thus, particularly weak effects are treated with caution in the interpretation, but the necessary measures have been taken to ensure the overall robustness of the results.

Beyond main effects, the choice and number of tested statistical interactions influence model interpretability and statistical power. To avoid overfitting, the spatial analysis focused on two biologically meaningful combinations with Julian day and precipitation and the respective presence of the other species. Only if the model containing the interaction showed a smaller AICc than the global model was the interaction included in the model selection. No interactions were tested in the temporal analysis, although some showed significance in the spatial analysis. This may have resulted in potentially relevant biological interactions remaining undetected. However, since only the intervals between one species pair were considered per model, the sample size was significantly reduced compared to the spatial analysis with additional daily variables (sin and cos (time)). Additional interactions could easily have led to overfitting. Nevertheless, the observed species- and scale-specific patterns indicate that biologically meaningful relationships were captured despite model simplifications.

For the temporal analysis, several methodological and statistical considerations apply due to the structure of inter-event data and pairwise comparisons. It should be noted that some of the direction-dependent inter-event intervals can be explained by different detection frequencies of the species (Sollmann, 2018; Ferry et al., 2024). If red deer are detected more frequently than roe deer or chamois, sequences of other species to red deer occur more frequently and closer together in time than the opposite direction, purely by chance (MacKenzie et al., 2002; Swinkels et al., 2023; Smith et al., 2023; Ferry et al., 2024). Key covariates such as environment, time of day and season, as well as location and year, were taken into account as effects and random effects, but an explicit correction of local activity, for example via relative abundance indices or rate-preserving null models (Ferry et al., 2024), was not part of the analysis plan. The directional effects are therefore interpreted associatively, with reference to the possibility of a base rate component. Roe deer–chamois showed the longest intervals (both directions), consistent with their different habitat preferences. At 250 m, roe deer $\rightarrow$ chamois intervals were longer than chamois $\rightarrow$ roe deer intervals, which is consistent with microhabitat and detection-related differences. Roe deer–red deer intervals were shorter at 250 m than at 1 km, together with increased presence probability and positive presence correlation, this suggests

higher densities or closer co-use at lower elevations. For roe deer, this could lead to fitness costs in the case of resource competition; whether this involves active avoidance or active displacement from corresponding areas remains open and requires supplementary data (e.g. vegetation/quality, individual fitness metrics such as Anderwald et al. (2016) for chamois, ibex and red deer).

Another important limitation of the study is the lack of time limits on the intervals analysed. Individual very long intervals can skew the predicted mean intervals and the effects acting on them upwards. For this reason, the detected time-of-day effects (sin and cos (time)) in particular are interpreted with caution and show that there is a diurnal pattern. Subsequent studies could describe and represent such patterns even more accurately by limiting very long intervals (e.g. by capping the maximum intervals as, Niedballa et al., 2019 and Marion et al., 2022).

Furthermore, the time interval analysis follows a time-to-first-event approach. Here, only the first subsequent event is examined, and the strength and duration of an effect are not separated. Newer approaches to recurrent event models would take all subsequent events into account and explicitly quantify the direction, strength, and duration of the effect (Ferry et al., 2024). Comparable works such as Swinkels et al. (2023) use the survival approach, in which censored intervals (e.g. camera failure or end of study) and competing events caused by the detection of third species are taken into account. An interval is thus considered 'observed without target event up to this point' instead of deleted. This further reduces bias due to data loss and distortion due to third species. This approach was not implemented in the study, so the time-to-first-event results provide initial indications of temporary decoupling of the species, but could be meaningfully deepened and supported by the implementation of such approaches. Due to time constraints, these approaches were not included in this work. However, the linear modelling of AB BA intervals with the inclusion of covariates, on different camera grids and with a very large sample size can still be seen as sufficient power to interpret the results as temporal partitioning (Niedballa et al., 2019). This approach in the simulations tested by Niedballa et al. (2019) corresponds to the most powerful standard there. While more advanced recurrent-event or survival approaches could provide refined insights, the present design represents a validated and statistically powerful framework for detecting temporal partitioning patterns.

The computational capacity of the available hardware restricted more extensive model testing. This trade-off between complexity and feasibility was addressed by focusing on the most ecologically meaningful predictors and robust modelling approaches. By combining two research scales in the same study area with a large sample size over four years and a robust GLMM structure, this study picks up on similar studies on temporal and spatial partitioning. For example, Kavčić et al. (2021) discussed that a smaller spatial frame and a larger sample size could have revealed possible intraspecific interactions more clearly in their study. These methodological considerations suggest that the observed spatial and temporal patterns are not only artefacts of modelling, but likely reflect genuine ecological mechanisms, which are discussed in the following section.

4.5 Ecological implications

Based on the spatial and temporal results, while keeping methodological limitations in mind, several ecological implications can be derived regarding coexistence mechanisms, competitive interactions and potential future dynamics among alpine ungulates. Discussing these implications helps to link the observed statistical patterns to ecological processes and to evaluate how competition, habitat use and behavioural adjustments shape species assemblages in alpine ecosystems. The following section therefore outlines the main ecological interpretations and perspectives, beginning with data requirements for future studies, followed by resource-based mechanisms, competition and predator effects. First of all, future studies using experimental or controlled designs would be needed to more conclusively separate habitat effects from direct interspecific interactions. However, this could be challenging in the study area used.

Secondly, the spatial and temporal models considered broad-scale predictors, yet finer environmental variables such as vegetation quality, primary productivity or soil nutrient content may further explain habitat preferences. Studies such as Anderwald et al. (2016) demonstrated

that productivity gradients can influence habitat selection in chamois and ibex. Incorporating comparable measures for red and roe deer would therefore help to clarify whether observed overlaps or separation result from resource availability rather than behavioural avoidance. Integrating such fine-scale data could improve ecological interpretability of the models and reveal additional niche differentiation mechanisms. However, these remote sensing data do not exist for forested areas, or are difficult to collect.

Even without evidence of spatial displacement, competition can still have fitness-relevant consequences for subordinate species. Resource competition may manifest as reduced access to high-quality forage or as temporal segregation around shared feeding sites (Anderwald et al., 2015, 2016). Especially towards the end of summer and in early autumn, sufficient nutrient intake is crucial for rebuilding body condition before winter (Parker et al., 2009; Willisch et al., 2013; Brivio et al., 2019). If interference competition occurs during this critical period, it can lead to reduced growth or survival of juveniles, and possibly to long-term demographic weakening of the affected population. Chirichella et al. (2013) showed that chamois may exploit energetically poorer refuge microhabitats for foraging rather than shifting broad-scale spatial or temporal habitat use when competition increases. This underlines that coexistence without spatial segregation does not necessarily imply the absence of competition, but rather reflects behavioural adjustment under resource limitation. Such mechanisms may become particularly important for mountain species that are physiologically constrained by temperature. Additional competition pressure could amplify the effects of climate change (van Beest et al., 2012; Ferretti et al., 2019).

Climate change and the expected increase in extreme weather events are likely to alter both intra- and interspecific interactions among alpine ungulates (Brivio et al., 2019). According to Anderwald et al. (2024), chamois respond to high temperatures not only by moving to higher elevations, but also by shifting into areas with greater tree cover. Those are habitats more typical for lower-elevation species such as red deer. Such behavioural plasticity could increase spatial and temporal overlap between these species. This could intensify competition for thermally suitable and productive foraging sites (de Frenne et al., 2019; Widén et al., 2025). While direct evidence for this mechanism in chamois is lacking, high summer temperatures lead chamois to select more forested, shaded sites (Anderwald et al., 2024), and forests buffer thermal extremes (de Frenne et al., 2019). By analogy to overcrowding observed in other alpine ungulates at high elevations (Brivio et al., 2019), such concentration in limited refuge areas could increase intra- and interspecific competition and may reduce access to high-quality forage (Widén et al., 2025). This remains a hypothesis to be tested. Similar processes may apply to red deer, where droughts and reduced forage productivity could increase density-dependent competition in forested valley bottoms (Widén et al., 2025). Overall, the combined effects of warming, habitat compression and changing vegetation structure may enhance competitive pressure among sympatric ungulates in the Alps (van Beest et al., 2012; de Frenne et al., 2019; Ferretti et al., 2019; Anderwald et al., 2024).

Additionally expansion of large carnivores such as the grey wolf and brown bear may alter these interspecific dynamics (Bleicher, 2017; Stears et al., 2020; Dellinger et al., 2022). According to Šprem et al. (2015), chamois in forested habitats exhibited clear shifts in activity patterns to avoid predators, mainly wolves, which overrode potential competition effects with other ungulates such as wild boar. Similarly, increasing predator presence in the Alps could either buffer herbivore competition by inducing shared avoidance behaviour (De Boer and Prins, 1990; Stears et al., 2020), or intensify temporal segregation among prey species through cascading effects on activity patterns (Dellinger et al., 2022). Monitoring these changes in parallel with herbivore interactions will be crucial for understanding future community structuring in alpine systems.

Chapter 5

Conclusion

The spatial presence of roe deer, chamois and red deer in the Il Fuorn area of the Swiss National Park is primarily influenced by environmental conditions and resource availability. No evidence was found for spatial displacement of roe deer or chamois by red deer. However, supplementary temporal interval analyses carried out at the same location indicate asymmetric, temporally mediated interactions: roe deer and chamois avoid red deer events temporally as there were longer intervals after red deer detections than in the opposite direction. This represents a pattern of behaviourally mediated coexistence without spatial segregation. The results provide a robust basis for locating competitive processes in the system temporally rather than spatially, and are therefore directly relevant for future studies of multi-species interactions and for monitoring and management decisions in alpine ecosystems. Understanding these interactions is essential for predicting how ongoing climate change and predator recolonisation may reshape alpine ungulate communities and for developing adaptive management strategies in protected mountain areas.

List of References

Akaike, H. (1973). Information theory as an extension of the maximum likelihood principle. In *Petrov, B. N. and Csaki, F. (Eds.), Second International Symposium on Information Theory. Akademiai Kiado, Budapest, pp. 276–281.*

Anderwald, P., S. Buchmann, T. Rempfler, and F. Filli (2024). Weather-dependent changes in habitat use by alpine chamois. *Movement Ecology 12*(3).

Anderwald, P., R. M. Haller, and F. Filli (2016). Heterogeneity in primary productivity influences competitive interactions between red deer and alpine chamois. *PLoS ONE 11*(1), e0146458.

Anderwald, P., I. Herfindal, R. M. Haller, A. C. Risch, M. Schütz, A. K. Schweiger, and F. Filli (2015). Influence of migratory ungulate management on competitive interactions with resident species in a protected area. *Ecosphere 6*(11), 1–18.

Andreoli, E., C. Roncoroni, F. Gusmeroli, G. Della Marianna, G. Giacometti, M. Heroldová, S. Barbieri, and S. Mattiello (2016). Feeding ecology of alpine chamois living in sympatry with other ruminant species. *Wildlife Biology 22*(3), 78–85.

Apollonio, M., R. Andersen, and R. Putman (2010). *European Ungulates and Their Management in the 21st Century*. Cambridge University Press.

Arnold, T. W. (2010). Uninformative parameters and model selection using Akaike's Information Criterion. *The Journal of Wildlife Management 74*(6), 1175–1178.

Bartoń, K. (2025). *MuMIn: Multi-Model Inference*. R package version 1.48.11.

Blanchet, F. G., K. Cazelles, and D. Gravel (2020). Co-occurrence is not evidence of ecological interactions. *Ecology Letters 23*(7), 1050–1063.

Bleicher, S. S. (2017). The landscape of fear conceptual framework: definition and review of current applications and misuses. *PeerJ 5*, e3772.

Borkowski, J., R. Banul, J. Jurkiewicz, C. Hołdyński, J. Świeczkowska, M. Nasiadko, and D. Załuski (2019). High density of keystone herbivore vs. conservation of natural resources: Factors affecting red deer distribution and impact on vegetation in słowiński national park, poland. *Forest Ecology and Management 450*, 117503.

Borkowski, J., R. Banul, J. Jurkiewicz-Azab, C. Hołdyński, J. Święczkowska, M. Nasiadko, and D. Załuski (2021). There is only one winner: The negative impact of red deer density on roe deer numbers and distribution in the Słowiński National Park and its vicinity. *Ecology and Evolution 11*(11), 6889–6899.

Brivio, F., M. Zurmühl, S. Grignolio, J. von Hardenberg, M. Apollonio, and S. Ciuti (2019). Forecasting the response to global warming in a heat-sensitive species. *Scientific Reports 9*(1), 3048.

Brooks, M. E., K. Kristensen, K. J. van Benthem, A. Magnusson, C. W. Berg, A. Nielsen, H. J. Skaug, M. Mächler, and B. M. Bolker (2017). glmmtmb balances speed and flexibility among packages for zero-inflated generalized linear mixed modeling. *The R Journal 9*(2), 378–400. R package version 0.2.0.

Burnham, K. P. and D. R. Anderson (Eds.) (2004). *Model Selection and Multimodel Inference*. New York: Springer NY.

Burton, A. C., E. Neilson, D. Moreira, A. Ladle, R. Steenweg, J. T. Fisher, E. Bayne, and S. Boutin (2015). Wildlife camera trapping: a review and recommendations for linking surveys to ecological processes. *Journal of Applied Ecology 52*(3), 675–685.

Chirichella, R., S. Ciuti, and M. Apollonio (2013). Effects of livestock and non-native mouflon on use of high-elevation pastures by alpine chamois. *Mammalian Biology 78*(5), 344–350.

Corlatti, L., A. Bonardi, N. Bragalanti, and L. Pedrotti (2019). Long-term dynamics of alpine ungulates suggest interspecific competition. *Journal of Zoology 309*(4), 241–249.

Cromsigt, J. P. G. M. and H. Olff (2006). Resource partitioning among savanna grazers mediated by local heterogeneity: An experimental approach. *Ecology 87*(6), 1532–1541.

Darmon, G., C. Calenge, A. Loison, J.-M. Jullien, D. Maillard, and J.-F. Lopez (2012). Spatial distribution and habitat selection in coexisting species of mountain ungulates. *Ecography 35*(1), 44–53.

De Boer, W. F. and H. H. T. Prins (1990). Large herbivores that strive mightily but eat and drink as friends. *Oecologia 82*(2), 264–274.

de Frenne, P., F. Zellweger, F. Rodríguez-Sánchez, B. R. Scheffers, K. Hylander, M. Luoto, M. Vellend, K. Verheyen, and J. Lenoir (2019). Global buffering of temperatures under forest canopies. *Nature Ecology & Evolution 3*(5), 744–749.

DeepL (2025). DeepL Translator. `https://www.deepl.com/translator`. Accessed: November 2025.

Dellinger, J. A., C. R. Shores, A. D. Craig, S. M. Kachel, M. R. Heithaus, W. J. Ripple, and A. J. Wirsing (2022). Predators reduce niche overlap between sympatric prey. *Oikos 2022*(1).

Di Bitetti, M. S., C. D. de Angelo, Y. E. Di Blanco, and A. Paviolo (2010). Niche partitioning and species coexistence in a neotropical felid assemblage. *Acta Oecologica 36*(4), 403–412.

Donini, V., L. Pedrotti, F. Ferretti, E. Iacona, L. Lorenzetti, F. Cozzi, and L. Corlatti (2025). Spatial and temporal relationships between roe and red deer in an alpine area. *Ecology and Evolution 15*(1), e70777.

Dormann, C. F., M. Bobrowski, D. M. Dehling, D. J. Harris, F. Hartig, H. Lischke, M. D. Moretti, J. Pagel, S. Pinkert, M. Schleuning, S. I. Schmidt, C. S. Sheppard, M. J. Steinbauer, D. Zeuss, and C. Kraan (2018). Biotic interactions in species distribution modelling: 10 questions to guide interpretation and avoid false conclusions. *Global Ecology and Biogeography 27*(9), 1004–1016.

Dormann, C. F., J. Elith, S. Bacher, C. Buchmann, G. Carl, G. Carré, J. R. García Marquéz, B. Gruber, B. Lafourcade, P. J. Leitão, T. Münkemüller, C. McClean, P. E. Osborne, B. Reineking, B. Schröder, A. K. Skidmore, D. Zurell, and S. Lautenbach (2013). Collinearity: a review of methods to deal with it and a simulation study evaluating their performance. *Ecography 36*(1), 27–46.

Durant, S. M. (1998). Competition refuges and coexistence: an example from Serengeti carnivores. *Journal of Animal Ecology 67*(3), 370–386.

Federal Office of Meteorology and Climatology MeteoSwiss (2025). Meteorological station data from Buffalora (tre200h0, rre150h0, rre024i0, tre200dx, tre200dn). `https://www.meteoswiss.admin.ch/`. Accessed via IDAweb. Times in UTC; data status summer 2025.

Federal Office of Topography (swisstopo) (2024a). *The high precision digital elevation model of Switzerland swissALTI3D*. Wabern, Switzerland: swisstopo. Digital elevation model swissALTI3D, LV95 LN02, 2024 version.

Federal Office of Topography (swisstopo) (2024b). *Swiss Map Raster 500 – Digital National Map of Switzerland 1:500,000*. Wabern, Switzerland: swisstopo. Georeferenced raster map, CH1903+/LV95, 2024 version.

Federal Office of Topography (swisstopo) (2024c). swisssurface3d – classified point cloud of switzerland. Classified LiDAR point cloud, 1 km2 tiles, 2024 edition.

Ferretti, F., S. Lovari, and P. A. Stephens (2019). Joint effects of weather and interspecific competition on foraging behavior and survival of a mountain herbivore. *Current Zoology 65*(2), 165–175.

Ferretti, F., A. Sforzi, and S. Lovari (2008). Intolerance amongst deer species at feeding: roe deer are uneasy banqueters. *Behavioural Processes 78*(3), 487–491.

Ferry, N., P. Dupont, A. Bender, and M. Heurich (2024). Introducing recurrent event analyses to assess species interactions based on camera-trap data: A comparison with time-to-first-event approaches. *Methods in Ecology and Evolution 15*(7), 1233–1246.

Gillespie, R. G. (2024). Habitat and niche, concept of. In S. M. Scheiner (Ed.), *Encyclopedia of Biodiversity (Third Edition)*, pp. 99–111. Oxford: Academic Press.

Greenland, S., J. J. Schlesselman, and M. H. Criqui (1986). The fallacy of employing standardized regression coefficients and correlations as measures of effect. *American Journal of Epidemiology 123*(2), 203–208.

Haller, H. (2002). *Der Rothirsch im Schweizerischen Nationalpark und dessen Umgebung: Eine alpine Population von Cervus elaphus zeitlich und räumlich dokumentiert: Zugl.: Zürich, Univ., Diss., 2000-2001*, Volume Nr. 91 of *Nationalpark-Forschung in der Schweiz*. Zernez and Göttingen: Schweizerischer Nationalpark and Inst. für Wildbiologie und Jagdkunde.

Hartig, F. (2024). *DHARMa: Residual Diagnostics for Hierarchical (Multi-Level / Mixed) Regression Models*. R package version 0.4.7.

Hemami, M.-R., A. R. Watkinson, and P. M. Dolman (2005). Population densities and habitat associations of introduced muntjac muntiacus reevesi and native roe deer capreolus capreolus in a lowland pine forest. *Forest Ecology and Management 215*(1-3), 224–238.

Hijmans, R. J. (2025). *terra: Spatial Data Analysis*. R package version 1.8-67.

Holdridge, E. M., C. Cuellar-Gempeler, and C. P. terHorst (2016). A shift from exploitation to interference competition with increasing density affects population and community dynamics. *Ecology and Evolution 6*(15), 5333–5341.

IUCN (2025). Swiss National Park - IUCN Green List. Accessed: June 2025.

Jelinski, D. E. and J. Wu (1996). The modifiable areal unit problem and implications for landscape ecology. *Landscape Ecology 11*(3), 129–140.

Johnson, A. S., P. E. Hale, W. M. Ford, J. M. Wentworth, J. R. French, O. F. Anderson, and G. B. Pullen (1995). White-tailed deer foraging in relation to successional stage, overstory type and management of southern appalachian forests. *American Midland Naturalist 133*(1), 18–35.

Kavčić, K., T. Radočaj, L. Corlatti, T. Safner, A. Gračanin, K. M. Mikac, and N. Šprem (2021). Spatio-temporal response of forest-dwelling chamois to red deer presence. *Mammalian Biology 101*(6), 907–915.

Krebs, C. J. (2001). *Ecology: The experimental analysis of distribution and abundance. Part 3 The Problem of Abundance: Populations* (5th ed.). San Francisco: Benjamin Cummings.

Latham, J., B. W. Staines, and M. L. Gorman (1996). The relative densities of red (Cervus elaphus) and roe (Capreolus capreolus) deer and their relationship in scottish plantation forests. *Journal of Zoology 240*(2), 285–299.

Latham, J., B. W. Staines, and M. L. Gorman (1999). Comparative feeding ecology of red (cervus elaphus) and roe deer (capreolus capreolus) in scottish plantation forests. *Journal of Zoology 247*(3), 409–418.

Lenth, R. V. (2025a). *emmeans: Estimated Marginal Means, aka Least-Squares Means.* R package version 1.11.2-8.

Lenth, R. V. (2025b). Transformations and link functions (emmeans vignette). CRAN vignette. R package: emmeans version 1.11.2-8.

Lotz, A. (2006). Alpine habitat diversity HABITALP. 2002-2006. Project report, EU Community Initiative Interreg III B Alpine Space Programme, Berchtesgaden, Germany.

Lovari, S., F. Ferretti, M. Corazza, I. Minder, N. Troiani, C. Ferrari, and A. Saddi (2014). Unexpected consequences of reintroductions: competition between reintroduced red deer and apennine chamois. *Animal Conservation 17*(4), 359–370.

MacKenzie, D. I., L. L. Bailey, and J. D. Nichols (2004). Investigating species co-occurrence patterns when species are detected imperfectly. *Journal of Animal Ecology 73*(3), 546–555.

MacKenzie, D. I., J. D. Nichols, G. B. Lachman, S. Droege, J. Andrew Royle, and C. A. Langtimm (2002). Estimating site occupancy rates when detection probabilities are less than one. *Ecology 83*(8), 2248–2255.

Mancinelli, S., Peters, W., Boitani, L., Hebblewhite, M., and Cagnacci, F. (2015). Roe deer summer habitat selection at multiple spatio-temporal scales in an alpine environment. *Hystrix, the Italian Journal of Mammalogy 26*(2), 132–140.

Marion, S., U. Demšar, A. L. Davies, P. A. Stephens, R. J. Irvine, and J. A. Long (2022). Spatial and temporal variations in interspecific interaction: impact of a recreational landscape. *European Journal of Wildlife Research 68*(36).

Marshall, H. E., N. Sukumal, D. Ngoprasert, and T. Savini (2023). The spatial and temporal displacement of native species by domestic dogs. *Global Ecology and Conservation 44*, e02504.

Nakagawa, S., P. C. D. Johnson, and H. Schielzeth (2017). The coefficient of determination R^2 and intra-class correlation coefficient from generalized linear mixed-effects models revisited and expanded. *Journal of the Royal Society, Interface 14*(134).

Ngoprasert, D., R. Steinmetz, K. Sribuarod, and G. A. Gale (2022). The overlap of sympatric sun bears and asiatic black bears in space and time. *Mammalian Biology 102*(1), 143–153.

Niedballa, J., A. Wilting, R. Sollmann, H. Hofer, and A. Courtiol (2019). Assessing analytical methods for detecting spatiotemporal interactions between species from camera trapping data. *Remote Sensing in Ecology and Conservation 5*(3), 272–285.

Parker, K. L., P. S. Barboza, and M. P. Gillingham (2009). Nutrition integrates environmental responses of ungulates. *Functional Ecology 23*(1), 57–69.

QGIS Development Team (2025). *QGIS Geographic Information System, Version 3.42 "Münster"*. QGIS Association. Release 3.42 "Münster".

R Core Team (2021). *R: A Language and Environment for Statistical Computing.* Vienna, Austria: R Foundation for Statistical Computing. Version 4.1.2, and 4.5.0.

Ramesh, T., R. Kalle, and C. T. Downs (2017). Staying safe from top predators: patterns of co-occurrence and inter-predator interactions. *Behavioral Ecology and Sociobiology 71*(2).

Richards, S. A., M. J. Whittingham, and P. A. Stephens (2011). Model selection and model averaging in behavioural ecology: the utility of the it-aic framework. *Behavioral Ecology and Sociobiology 65*(1), 77–89.

Schielzeth, H. (2010). Simple means to improve the interpretability of regression coefficients. *Methods in Ecology and Evolution 1*(2), 103–113.

Schoener, T. W. (1973). Population growth regulated by intraspecific competition for energy or time: some simple representations. *Theoretical Population Biology 4*(1), 56–84.

Schweizerischer Nationalpark (2019). Kapitel 9: Natur. In *Geschäftsbericht 2018*, pp. 44–55. Zernez, Schweiz: Eidgenössische Nationalparkkommission (enpk) und Stiftung Schweizerischer Nationalpark Zernez.

Schweizerischer Nationalpark (2020). Kapitel 9: Natur. In *Geschäftsbericht 2019*, pp. 47–57. Zernez, Schweiz: Eidgenössische Nationalparkkommission (enpk) und Stiftung Schweizerischer Nationalpark Zernez.

Schweizerischer Nationalpark (2021). Kapitel 9: Natur. In *Geschäftsbericht 2020*, pp. 53–64. Zernez, Schweiz: Eidgenössische Nationalparkkommission (enpk) und Stiftung Schweizerischer Nationalpark Zernez.

Schweizerischer Nationalpark (2024). Über den schweizerischen nationalpark. `https://www.nationalpark.ch/about/nationalpark/`. Accessed: June 2025.

Semper-Pascual, A., D. Sheil, L. Beaudrot, P. Dupont, S. Dey, J. Ahumada, E. Akampurira, R. Bitariho, S. Espinosa, P. A. Jansen, M. G. M. Lima, E. H. Martin, B. Mugerwa, F. Rovero, F. Santos, E. Uzabaho, and R. Bischof (2023). Occurrence dynamics of mammals in protected tropical forests respond to human presence and activities. *Nature Ecology & Evolution 7*(7), 1092–1103.

Smith, K., J. A. Venter, M. Peel, M. Keith, and M. J. Somers (2023). Temporal partitioning and the potential for avoidance behaviour within South African carnivore communities. *Ecology and Evolution 13*(8), e10380.

Sollmann, R. (2018). A gentle introduction to camera-trap data analysis. *African Journal of Ecology 56*(4), 740–749.

Šprem, N., D. Zanella, D. Ugarković, I. Prebanić, P. Gančević, and L. Corlatti (2015). Unimodal activity pattern in forest-dwelling chamois: typical behaviour or interspecific avoidance? *European Journal of Wildlife Research 61*(5), 789–794.

Stears, K., M. H. Schmitt, C. C. Wilmers, and A. M. Shrader (2020). Mixed-species herding levels the landscape of fear. *Proceedings of the Royal Society B: Biological Sciences 287*(1922), 20192555.

Storms, D., P. Aubry, J.-L. Hamann, S. Saïd, H. Fritz, C. Saint-Andrieux, and F. Klein (2008). Seasonal variation in diet composition and similarity of sympatric red deer (Cervus elaphus) and roe deer (Capreolus capreolus). *Wildlife Biology 14*(2), 237–250.

Swinkels, C., J. E. M. van der Wal, C. Stinn, C. M. Monteza-Moreno, and P. A. Jansen (2023). Prey tracking and predator avoidance in a neotropical moist forest: a camera-trapping approach. *Journal of Mammalogy 104*(1), 137–145.

Symonds, M. R. E. and A. Moussalli (2011). A brief guide to model selection, multimodel inference and model averaging in behavioural ecology using akaike's information criterion. *Behavioral Ecology and Sociobiology 65*(1), 13–21.

Tallian, A., A. Ordiz, M. C. Metz, B. Zimmermann, C. Wikenros, D. W. Smith, D. R. Stahler, P. Wabakken, J. E. Swenson, H. Sand, and J. Kindberg (2022). Of wolves and bears: Seasonal drivers of interference and exploitation competition between apex predators. *Ecological Monographs 92*(2).

Timcke, J. (2025). Roe deer responses to recolonising wolves: automated camera trap approaches in the Swiss National Park. Master's thesis, ETH Zürich, Zürich, Switzerland. MSc thesis.

Torres, R. T., E. Virgós, J. Santos, J. D. Linnell, and C. Fonseca (2012). Habitat use by sympatric red and roe deer in a Mediterranean ecosystem. *Animal Biology 62*(3), 351–366.

van Beest, F. M., B. van Moorter, and J. M. Milner (2012). Temperature-mediated habitat use and selection by a heat-sensitive northern ungulate. *Animal Behaviour 84*(3), 723–735.

Wagner, F. H., W. L. Hamilton, and R. B. Keigley (2006). *Yellowstone's Destabilized Ecosystem: Elk effects, science, and policy conflict.* Oxford: Oxford University Press New York.

Wickham, H. (2016). *ggplot2: Elegant Graphics for Data Analysis.* Springer-Verlag New York. R package version 4.0.1.

Widén, A., J. P. G. M. Cromsigt, A. M. Felton, F. Widemo, L. Graf, G. Ericsson, and N. J. Singh (2025). Temperature mediated habitat selection in sympatric deer species with varying body size: thermal cover and forage availability as potential drivers. *Movement Ecology 13*(1), 52.

Willisch, C. S., K. Bieri, M. Struch, R. Franceschina, R. Schnidrig-Petrig, and P. Ingold (2013). Climate effects on demographic parameters in an unhunted population of alpine chamois (Rupicapra rupicapra). *Journal of Mammalogy 94*(1), 173–182.

Zoller, H. (1995). *Vegetationskarte des Schweizerischen Nationalparks: Erläuterungen.* Number 85 in Nationalpark-Forschung in der Schweiz. Zernez: Nationalparkhaus.

Appendix A

Biological relevance for tested interactions in the spatial analysis

A.1 Precipitation x Species presence

Precipitation can have a significant impact on the spatial and habitat use of mountain ungulates. In particular in the Alpine region, where there is heavy rainfall in exposed terrain, species such as chamois move to more sheltered areas (de Frenne et al., 2019; van Beest et al., 2012; Anderwald et al., 2024). This can increase spatial overlap with other ungulate species. The spatial use of roe deer and red deer (Apollonio et al., 2010; Borkowski et al., 2021), as well as chamois and red deer (Lovari et al., 2014), already show considerable overlap and are strongly influenced by environmental factors. If chamois for example tend to stay in wooded areas during heavy rainfall (Anderwald et al., 2024), but are present in higher, rockier areas when red deer are more abundant (Anderwald et al., 2015), these two effects could influence each other. An interaction between the presence of a potentially competing species and precipitation allows to test whether the influence of the presence of the potentially competing species on the presence of the target species is precipitation-dependent (and, conversely, whether the effect of precipitation changes in the presence of the competing species).

A.2 Julian day x Species presence

During the course of the year, environmental conditions (vegetation changes, snow cover, average temperatures) as well as habitat use and activity patterns or foraging behaviour(Storms et al., 2008; Parker et al., 2009; Kavčić et al., 2021; Widén et al., 2025) of the species studied, change. Sympatric species can adapt their spatial and temporal use over the course of the year, thereby alter competitive situations (Kavčić et al., 2021; Tallian et al., 2022; Smith et al., 2023). An interaction between Julian day and the presence of a potentially competing species covers the fact that the strength of the competitive effect can vary seasonally (Tallian et al., 2022). Therefore, it is not necessary to specify a separate interaction for each individual variable with seasonal change. By focusing on these two important potential factors influencing partitioning behaviour, the risk of overfitting can be avoided while still taking relevant interactions between covariates into account.

Appendix B

Correlation matrices (Spearman)

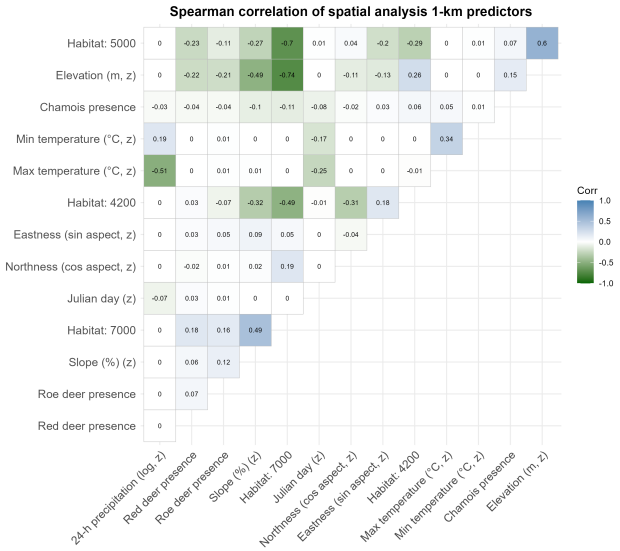

(a) 1 km – spatial

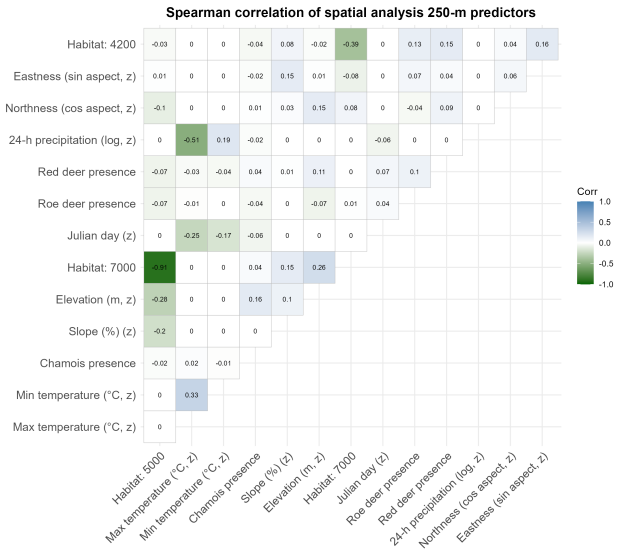

(b) 250 m – spatial

Figure B.1: Spearman correlations for the spatial models.

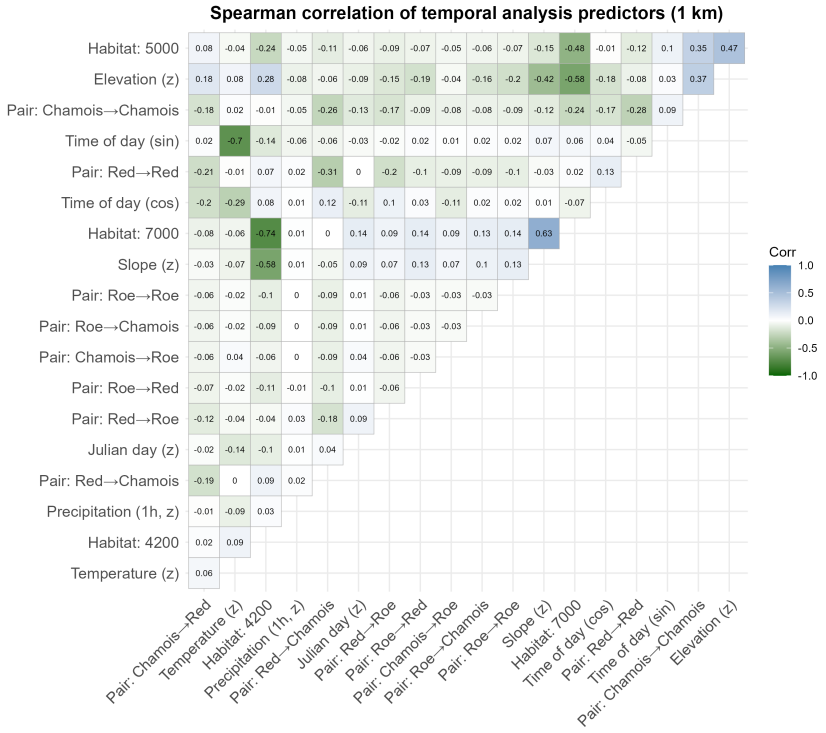

(a) 1 km – temporal

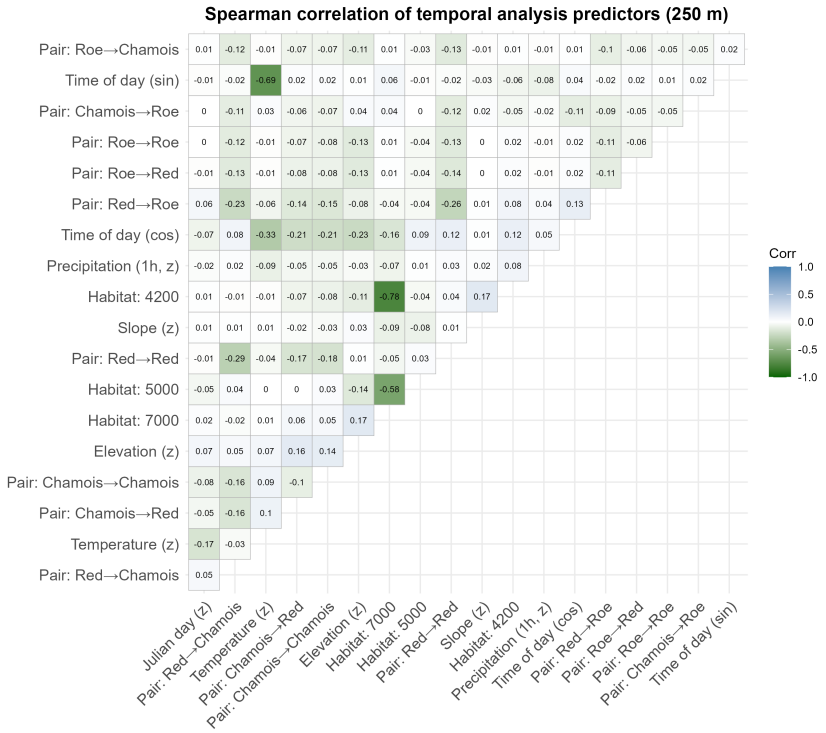

(b) 250 m – temporal

Figure B.2: Spearman correlations for the temporal models.

Appendix C

Top models summary

C.1 Spatial analysis Top models

C.1.1 Spatial roe deer 1 km

Table C.1: Top models (ΔAICc ≤ 2) used for model averaging for the roe deer GLMM (1 km). All models include an intercept and random intercepts for *Location* and *trapdays*; `ziformula = ~0`, `dispformula = ~1`.

Model	k	logLik	AICc	ΔAICc	Weight	Predictors (fixed effects)
1	5	-1749.94	3509.88	0.00	0.06	Elevation (z) + Min temperature (z)
2	7	-1748.01	3510.03	0.15	0.05	Habitat type + Elevation (z) + Min temperature (z)
3	4	-1751.23	3510.47	0.58	0.04	Elevation (z)
4	6	-1749.27	3510.54	0.65	0.04	Elevation (z) + Julian day (z) + Min temperature (z)
5	6	-1749.30	3510.61	0.73	0.04	Habitat type + Elevation (z)
6	8	-1747.34	3510.68	0.80	0.04	Habitat type + Elevation (z) + Julian day (z) + Min temperature (z)
7	6	-1749.48	3510.95	1.07	0.03	Elevation (z) + Min temperature (z) + Slope (z)
8	6	-1749.49	3510.98	1.09	0.03	Elevation (z) + Min temperature (z) + Red deer presence
9	8	-1747.52	3511.04	1.16	0.03	Habitat type + Elevation (z) + Min temperature (z) + Northness (cos aspect, z)
10	8	-1747.56	3511.14	1.25	0.03	Habitat type + Elevation (z) + Min temperature (z) + Red deer presence
11	6	-1749.60	3511.20	1.31	0.03	Elevation (z) + Min temperature (z) + Northness (cos aspect, z)
12	5	-1750.63	3511.27	1.38	0.03	Elevation (z) + Max temperature (z)
13	7	-1748.71	3511.42	1.53	0.03	Habitat type + Elevation (z) + Max temperature (z)
14	8	-1747.75	3511.51	1.62	0.03	Habitat type + Elevation (z) + Min temperature (z) + Slope (z)
15	5	-1750.77	3511.54	1.65	0.03	Elevation (z) + Slope (z)
16	6	-1749.77	3511.54	1.66	0.03	Chamois presence + Elevation (z) + Min temperature (z)
17	6	-1749.79	3511.58	1.70	0.03	Elevation (z) + Max temperature (z) + Min temperature (z)
18	9	-1746.84	3511.69	1.80	0.02	Habitat type + Elevation (z) + Julian day (z) + Min temperature (z) + Northness (cos aspect, z)
19	6	-1749.86	3511.72	1.84	0.02	Elevation (z) + Min temperature (z) + 24-h precipitation (log, z)
20	5	-1750.86	3511.73	1.85	0.02	Elevation (z) + Julian day (z)
21	8	-1747.86	3511.73	1.85	0.02	Habitat type + Elevation (z) + Max temperature (z) + Min temperature (z)
22	5	-1750.89	3511.78	1.90	0.02	Elevation (z) + Northness (cos aspect, z)
23	7	-1748.89	3511.78	1.90	0.02	Elevation (z) + Julian day (z) + Min temperature (z) + Red deer presence

Continued on next page

Model	k	logLik	AICc	ΔAICc	Weight	Predictors (fixed effects)
24	6	-1749.89	3511.79	1.91	0.02	Eastness (sin aspect, z) + Elevation (z) + Min temperature (z)
25	7	-1748.90	3511.81	1.93	0.02	Elevation (z) + Julian day (z) + Max temperature (z) + Min temperature (z)
26	7	-1748.90	3511.82	1.93	0.02	Habitat type + Elevation (z) + Red deer presence
27	7	-1748.92	3511.85	1.96	0.02	Elevation (z) + Julian day (z) + Min temperature (z) + Northness (cos aspect, z)
28	8	-1747.93	3511.87	1.99	0.02	Habitat type + Elevation (z) + Min temperature (z) + 24-h precipitation (log, z)
29	7	-1748.93	3511.87	1.99	0.02	Habitat type + Elevation (z) + Julian day (z)
				Cumulative weight		0.06, 0.11, 0.15, 0.19, 0.23, 0.27, 0.30, 0.33, 0.36, 0.39, 0.42, 0.45, 0.48, 0.51, 0.54, 0.57, 0.59, 0.61, 0.63, 0.65, 0.67, 0.69, 0.71, 0.73, 0.75, 0.77, 0.79, 0.81, 0.83

C.1.2 Spatial roe deer 250 m

Table C.2: Top models (ΔAICc ≤ 2) used for model averaging for the roe deer GLMM (250 m). All models include an intercept and random intercepts for *Location* and *trapdays*; `ziformula = ~0`, `dispformula = ~1`.

Model	k	logLik	AICc	ΔAICc	Weight	Predictors (fixed effects)
1	9	-5009.68	10037.37	0.00	0.21	Habitat type + Elevation (z) + Julian day (z) + Min temperature (z) + Red deer presence
2	8	-5011.18	10038.36	1.00	0.13	Habitat type + Elevation (z) + Julian day (z) + Red deer presence
3	9	-5010.30	10038.61	1.24	0.11	Habitat type + Elevation (z) + Julian day (z) + Max temperature (z) + Red deer presence
4	10	-5009.36	10038.72	1.36	0.11	Habitat type + Elevation (z) + Julian day (z) + Min temperature (z) + 24-h precipitation (log, z) + Red deer presence
5	10	-5009.37	10038.74	1.38	0.10	Eastness (sin aspect, z) + Habitat type + Elevation (z) + Julian day (z) + Min temperature (z) + Red deer presence
6	10	-5009.37	10038.75	1.38	0.10	Habitat type + Elevation (z) + Julian day (z) + Max temperature (z) + Min temperature (z) + Red deer presence
7	10	-5009.62	10039.25	1.88	0.08	Habitat type + Elevation (z) + Julian day (z) + Min temperature (z) + Northness (cos aspect, z) + Red deer presence
8	10	-5009.64	10039.29	1.93	0.08	Habitat type + Elevation (z) + Julian day (z) + Min temperature (z) + Slope (z) + Red deer presence
9	10	-5009.65	10039.30	1.94	0.08	Chamois presence + Habitat type + Elevation (z) + Julian day (z) + Min temperature (z) + Red deer presence

C.1.3 Spatial chamois 1 km

Table C.3: Top models (ΔAICc $\leq$ 2) used for model averaging for the chamois GLMM (1 km). All models include an intercept and random intercepts for *Location* and *trapdays*; `ziformula = ~0`, `dispformula = ~1`.

Model	k	logLik	AICc	ΔAICc	Weight	Predictors (fixed effects)
1	10	-7185.20	14390.41	0.00	0.08	Eastness (sin aspect, z) + Elevation (z) + Julian day (z) + Slope (z) + 24-h precipitation (log, z) + Red deer presence + 24-h precipitation (log, z) × Red deer presence
2	9	-7186.23	14390.48	0.07	0.08	Eastness (sin aspect, z) + Elevation (z) + Julian day (z) + 24-h precipitation (log, z) + Red deer presence + 24-h precipitation (log, z) × Red deer presence
3	11	-7184.35	14390.71	0.31	0.07	Eastness (sin aspect, z) + Elevation (z) + Julian day (z) + Max temperature (z) + Slope (z) + 24-h precipitation (log, z) + Red deer presence + 24-h precipitation (log, z) × Red deer presence
4	10	-7185.39	14390.78	0.38	0.07	Eastness (sin aspect, z) + Elevation (z) + Julian day (z) + Max temperature (z) + 24-h precipitation (log, z) + Red deer presence + 24-h precipitation (log, z) × Red deer presence
5	8	-7187.40	14390.81	0.41	0.07	Elevation (z) + Julian day (z) + 24-h precipitation (log, z) + Red deer presence + 24-h precipitation (log, z) × Red deer presence
6	9	-7186.42	14390.85	0.44	0.06	Elevation (z) + Julian day (z) + Slope (z) + 24-h precipitation (log, z) + Red deer presence + 24-h precipitation (log, z) × Red deer presence
7	9	-7186.55	14391.12	0.71	0.06	Elevation (z) + Julian day (z) + Max temperature (z) + 24-h precipitation (log, z) + Red deer presence + 24-h precipitation (log, z) × Red deer presence
8	10	-7185.57	14391.15	0.74	0.06	Elevation (z) + Julian day (z) + Max temperature (z) + Slope (z) + 24-h precipitation (log, z) + Red deer presence + 24-h precipitation (log, z) × Red deer presence
9	11	-7184.63	14391.28	0.88	0.05	Eastness (sin aspect, z) + Elevation (z) + Julian day (z) + Min temperature (z) + Slope (z) + 24-h precipitation (log, z) + Red deer presence + 24-h precipitation (log, z) × Red deer presence
10	10	-7185.67	14391.36	0.95	0.05	Eastness (sin aspect, z) + Elevation (z) + Julian day (z) + Min temperature (z) + 24-h precipitation (log, z) + Red deer presence + 24-h precipitation (log, z) × Red deer presence
11	9	-7186.84	14391.69	1.28	0.04	Elevation (z) + Julian day (z) + Min temperature (z) + 24-h precipitation (log, z) + Red deer presence + 24-h precipitation (log, z) × Red deer presence
12	10	-7185.86	14391.72	1.32	0.04	Elevation (z) + Julian day (z) + Min temperature (z) + Slope (z) + 24-h precipitation (log, z) + Red deer presence + 24-h precipitation (log, z) × Red deer presence

Continued on next page

Model	k	logLik	AICc	ΔAICc	Weight	Predictors (fixed effects)
13	11	-7184.88	14391.78	1.38	0.04	Eastness (sin aspect, z) + Elevation (z) + Julian day (z) + Slope (z) + 24-h precipitation (log, z) + Roe deer presence + Red deer presence + 24-h precipitation (log, z) × Red deer presence
14	10	-7185.91	14391.84	1.43	0.04	Eastness (sin aspect, z) + Elevation (z) + Julian day (z) + 24-h precipitation (log, z) + Roe deer presence + Red deer presence + 24-h precipitation (log, z) × Red deer presence
15	12	-7184.03	14392.07	1.66	0.04	Eastness (sin aspect, z) + Elevation (z) + Julian day (z) + Max temperature (z) + Slope (z) + 24-h precipitation (log, z) + Roe deer presence + Red deer presence + 24-h precipitation (log, z) × Red deer presence
16	11	-7185.06	14392.13	1.72	0.03	Eastness (sin aspect, z) + Elevation (z) + Julian day (z) + Max temperature (z) + 24-h precipitation (log, z) + Roe deer presence + Red deer presence + 24-h precipitation (log, z) × Red deer presence
17	9	-7187.10	14392.20	1.80	0.03	Elevation (z) + Julian day (z) + 24-h precipitation (log, z) + Roe deer presence + Red deer presence + 24-h precipitation (log, z) × Red deer presence
18	10	-7186.12	14392.25	1.84	0.03	Elevation (z) + Julian day (z) + Slope (z) + 24-h precipitation (log, z) + Roe deer presence + Red deer presence + 24-h precipitation (log, z) × Red deer presence
19	11	-7185.14	14392.29	1.89	0.03	Eastness (sin aspect, z) + Elevation (z) + Julian day (z) + Slope (z) + 24-h precipitation (log, z) + Northness (cos aspect, z) + Red deer presence + 24-h precipitation (log, z) × Red deer presence
20	10	-7186.17	14392.36	1.95	0.03	Eastness (sin aspect, z) + Elevation (z) + Julian day (z) + 24-h precipitation (log, z) + Northness (cos aspect, z) + Red deer presence + 24-h precipitation (log, z) × Red deer presence
				Cumulative weight		0.08, 0.16, 0.23, 0.30, 0.37, 0.43, 0.49, 0.55, 0.60, 0.65, 0.69, 0.73, 0.77, 0.81, 0.85, 0.88, 0.91, 0.94, 0.97, 1.00

C.1.4 Spatial chamois 250 m

Table C.4: Top models (ΔAICc ≤ 2) used for model averaging for the chamois GLMM (250 m). All models include an intercept and random intercepts for *Location* and *trapdays*; `ziformula = ~0`, `dispformula = ~1`.

Model	k	logLik	AICc	ΔAICc	Weight	Predictors (fixed effects)
1	9	-6599.82	13217.64	0.00	0.28	Elevation (z) + Julian day (z) + Min temperature (z) + 24-h precipitation (log, z) + Red deer presence + Julian day (z) × Red deer presence
2	10	-6599.39	13218.79	1.15	0.16	Elevation (z) + Julian day (z) + Max temperature (z) + Min temperature (z) + 24-h precipitation (log, z) + Red deer presence + Julian day (z) × Red deer presence

Continued on next page

Model	k	logLik	AICc	ΔAICc	Weight	Predictors (fixed effects)
3	10	-6599.62	13219.24	1.60	0.12	Eastness (sin aspect, z) + Elevation (z) + Julian day (z) + Min temperature (z) + 24-h precipitation (log, z) + Red deer presence + Julian day (z) × Red deer presence
4	11	-6598.65	13219.32	1.67	0.12	Habitat type + Elevation (z) + Julian day (z) + Min temperature (z) + 24-h precipitation (log, z) + Red deer presence + Julian day (z) × Red deer presence
5	10	-6599.71	13219.42	1.78	0.11	Northness (cos aspect, z) + Elevation (z) + Julian day (z) + Min temperature (z) + 24-h precipitation (log, z) + Red deer presence + Julian day (z) × Red deer presence
6	10	-6599.78	13219.57	1.92	0.11	Elevation (z) + Julian day (z) + Min temperature (z) + 24-h precipitation (log, z) + Roe deer presence + Red deer presence + Julian day (z) × Red deer presence
7	10	-6599.81	13219.64	1.99	0.10	Elevation (z) + Julian day (z) + Min temperature (z) + Slope (z) + 24-h precipitation (log, z) + Red deer presence + Julian day (z) × Red deer presence
				Cumulative weight		0.28, 0.44, 0.56, 0.68, 0.79, 0.90, 1.00

C.1.5 Spatial red deer 1 km

Table C.5: Top models (ΔAICc ≤ 2) used for model averaging for the red deer GLMM (1 km). All models include an intercept and random intercepts for *Location* and *trapdays*; `ziformula = ~0`, `dispformula = ~1`.

Model	k	logLik	AICc	ΔAICc	Weight	Predictors (fixed effects)
1	9	−6687.14	13392.30	0.00	0.20	Chamois presence + Habitat type (factor) + Elevation (z) + Julian day (z) + Northness (cos aspect, z)
2	8	−6688.45	13392.91	0.62	0.15	Chamois presence + Habitat type (factor) + Elevation (z) + Julian day (z)
3	8	−6688.49	13393.00	0.70	0.14	Habitat type (factor) + Elevation (z) + Julian day (z) + Northness (cos aspect, z)
4	7	−6689.80	13393.61	1.31	0.10	Habitat type (factor) + Elevation (z) + Julian day (z)
5	10	−6686.88	13393.78	1.48	0.09	Chamois presence + Habitat type (factor) + Elevation (z) + Julian day (z) + Northness (cos aspect, z) + Roe deer presence
6	10	−6686.99	13393.99	1.70	0.09	Eastness (sin aspect, z) + Chamois presence + Habitat type (factor) + Elevation (z) + Julian day (z) + Northness (cos aspect, z)
7	10	−6687.04	13394.08	1.79	0.08	Chamois presence + Habitat type (factor) + Elevation (z) + Julian day (z) + Slope (z) + Northness (cos aspect, z)
8	10	−6687.12	13394.24	1.95	0.08	Chamois presence + Habitat type (factor) + Elevation (z) + Julian day (z) + Max temperature (z) + Northness (cos aspect, z)
9	10	−6687.14	13394.28	1.99	0.07	Chamois presence + Habitat type (factor) + Elevation (z) + Julian day (z) + 24-h precipitation (log, z) + Northness (cos aspect, z)

C.1.6 Spatial red deer 250 m

Table C.6: Top models (ΔAICc ≤ 2) used for model averaging for the red deer GLMM (250 m). All models include an intercept and random intercepts for *Location* and *trapdays*; `ziformula = ~0`, `dispformula = ~1`.

Model	k	logLik	AICc	ΔAICc	Weight	Predictors (fixed effects)
1	13	-10252.29	20530.60	0.00	0.15	Chamois presence + Habitat type + Elevation (z) + Julian day (z) + Min temperature (z) + 24-h precipitation (log, z) + Northness (cos aspect, z) + Roe deer presence + Chamois presence × Julian day (z)
2	12	-10253.36	20530.73	0.13	0.14	Chamois presence + Habitat type + Elevation (z) + Julian day (z) + Min temperature (z) + 24-h precipitation (log, z) + Roe deer presence + Chamois presence × Julian day (z)
3	13	-10252.72	20531.47	0.87	0.10	Chamois presence + Habitat type + Elevation (z) + Julian day (z) + Max temperature (z) + Min temperature (z) + Northness (cos aspect, z) + Roe deer presence + Chamois presence × Julian day (z)
4	12	-10253.76	20531.54	0.95	0.10	Chamois presence + Habitat type + Elevation (z) + Julian day (z) + Min temperature (z) + Northness (cos aspect, z) + Roe deer presence + Chamois presence × Julian day (z)
5	12	-10253.79	20531.60	1.00	0.09	Chamois presence + Habitat type + Elevation (z) + Julian day (z) + Min temperature (z) + Roe deer presence + Chamois presence × Julian day (z)
6	11	-10254.83	20531.68	1.08	0.09	Chamois presence + Habitat type + Elevation (z) + Julian day (z) + Min temperature (z) + Chamois presence × Julian day (z)
7	14	-10251.94	20531.90	1.30	0.08	Chamois presence + Habitat type + Elevation (z) + Julian day (z) + Min temperature (z) + Slope (z) + 24-h precipitation (log, z) + Northness (cos aspect, z) + Roe deer presence + Chamois presence × Julian day (z)
8	13	-10253.05	20532.13	1.53	0.07	Chamois presence + Habitat type + Elevation (z) + Julian day (z) + Min temperature (z) + Slope (z) + 24-h precipitation (log, z) + Roe deer presence + Chamois presence × Julian day (z)
9	14	-10252.20	20532.43	1.83	0.06	Chamois presence + Habitat type + Elevation (z) + Julian day (z) + Max temperature (z) + Min temperature (z) + 24-h precipitation (log, z) + Northness (cos aspect, z) + Roe deer presence + Chamois presence × Julian day (z)
10	13	-10253.27	20532.56	1.96	0.06	Chamois presence + Habitat type + Elevation (z) + Julian day (z) + Max temperature (z) + Min temperature (z) + 24-h precipitation (log, z) + Roe deer presence + Chamois presence × Julian day (z)

Continued on next page

Model	k	logLik	AICc	ΔAICc	Weight	Predictors (fixed effects)
11	14	-10252.28	20532.57	1.98	0.06	Eastness (sin aspect, z) + Chamois presence + Habitat type + Elevation (z) + Julian day (z) + Min temperature (z) + 24-h precipitation (log, z) + Northness (cos aspect, z) + Roe deer presence + Chamois presence × Julian day (z)
				Cumulative weight		0.15, 0.29, 0.39, 0.49, 0.58, 0.67, 0.75, 0.82, 0.88, 0.94, 1.00

C.2 Temporal analysis Top models

C.2.1 Roe deer, red deer 1 km

Table C.7: Top models (ΔAICc ≤ 2) used for model averaging for the roe deer, red deer GLMM (1 km). All models include an intercept and random intercepts for *Location* and *Year*; `ziformula = ~0`, `dispformula = ~Julian_day_z + Elevation_z + 1`.

Model	k	logLik	AICc	ΔAICc	Weight	Predictors (fixed effects)
1	13	-32733.70	65493.50	0.00	0.09	Species pair + Elevation (z) + Julian day (z) + Time of day (cos) + Air temperature (z)
2	12	-32734.77	65493.64	0.14	0.08	Species pair + Elevation (z) + Julian day (z) + Air temperature (z)
3	11	-32735.86	65493.81	0.30	0.07	Species pair + Elevation (z) + Julian day (z) + Time of day (cos) + Air temperature (z)
4	10	-32736.89	65493.84	0.33	0.07	Species pair + Elevation (z) + Julian day (z) + Air temperature (z)
5	14	-32733.17	65494.46	0.96	0.05	Species pair + Elevation (z) + Julian day (z) + Slope (z) + Time of day (cos) + Air temperature (z)
6	13	-32734.23	65494.58	1.07	0.05	Species pair + Elevation (z) + Julian day (z) + Slope (z) + Air temperature (z)
7	12	-32735.33	65494.76	1.25	0.05	Species pair + Elevation (z) + Julian day (z) + Slope (z) + Time of day (cos) + Air temperature (z)
8	11	-32736.34	65494.77	1.26	0.05	Species pair + Elevation (z) + Julian day (z) + Slope (z) + Air temperature (z)
9	13	-32734.49	65495.09	1.58	0.04	Species pair + Julian day (z) + Slope (z) + Time of day (cos) + Air temperature (z)
10	15	-32732.48	65495.10	1.60	0.04	Species pair + Habitat type + Elevation (z) + Julian day (z) + Time of day (cos) + Air temperature (z)
11	12	-32735.51	65495.12	1.61	0.04	Species pair + Julian day (z) + Slope (z) + Air temperature (z)
12	14	-32733.55	65495.24	1.73	0.04	Species pair + Habitat type + Elevation (z) + Julian day (z) + Air temperature (z)
13	10	-32737.59	65495.25	1.74	0.04	Species pair + Elevation (z) + Julian day (z) + Time of day (cos) + Air temperature (z)
14	10	-32737.60	65495.26	1.76	0.04	Species pair + Julian day (z) + Slope (z) + Air temperature (z)
15	9	-32738.60	65495.26	1.76	0.04	Species pair + Elevation (z) + Julian day (z) + Air temperature (z)
16	12	-32735.59	65495.27	1.76	0.04	Species pair + Julian day (z) + Time of day (cos) + Air temperature (z)
17	11	-32736.62	65495.32	1.81	0.03	Species pair + Julian day (z) + Air temperature (z)

Continued on next page

Model	k	logLik	AICc	ΔAICc	Weight	Predictors (fixed effects)
18	11	-32736.62	65495.33	1.83	0.03	Species pair + Julian day (z) + Slope (z) + Time of day (cos) + Air temperature (z)
19	13	-32734.64	65495.39	1.88	0.03	Species pair + Habitat type + Elevation (z) + Julian day (z) + Time of day (cos) + Air temperature (z)
20	12	-32735.66	65495.42	1.91	0.03	Species pair + Habitat type + Elevation (z) + Julian day (z) + Air temperature (z)
21	9	-32738.70	65495.45	1.95	0.03	Species pair + Julian day (z) + Air temperature (z)
22	14	-32733.68	65495.49	1.99	0.03	Species pair + Elevation (z) + Julian day (z) + 1-h precipitation (z) + Time of day (cos) + Air temperature (z)
				Cumulative weight		0.09, 0.17, 0.24, 0.31, 0.36, 0.41, 0.46, 0.51, 0.55, 0.59, 0.63, 0.67, 0.71, 0.75, 0.79, 0.83, 0.86, 0.89, 0.92, 0.95, 0.98, 1.00

C.2.2 Roe deer, red deer 250 m

Table C.8: Top models (ΔAICc ≤ 2) used for model averaging for the roe deer, red deer GLMM (250 m). All models include an intercept and random intercepts for *Location* and *Year*; `ziformula = ~0`, `dispformula = ~Habitat type + Elevation_z + 1`.

Model	k	logLik	AICc	ΔAICc	Weight	Predictors (fixed effects)
1	14	-89684.80	179397.60	0.00	0.18	Species pair + Habitat type + Julian day (z) + Time of day (cos) + Time of day (sin) + Temperature (z)
2	13	-89685.85	179397.70	0.08	0.17	Species pair + Habitat type + Julian day (z) + Time of day (sin) + Temperature (z)
3	15	-89684.37	179398.80	1.15	0.10	Species pair + Habitat type + Julian day (z) + Precipitation (1h, z) + Time of day (cos) + Time of day (sin) + Temperature (z)
4	14	-89685.48	179399.00	1.36	0.09	Species pair + Habitat type + Julian day (z) + Precipitation (1h, z) + Time of day (sin) + Temperature (z)
5	15	-89684.54	179399.10	1.48	0.08	Species pair + Habitat type + Elevation (z) + Julian day (z) + Time of day (cos) + Time of day (sin) + Temperature (z)
6	15	-89684.59	179399.20	1.57	0.08	Species pair + Habitat type + Julian day (z) + Slope (z) + Time of day (cos) + Time of day (sin) + Temperature (z)
7	14	-89685.62	179399.30	1.63	0.08	Species pair + Habitat type + Elevation (z) + Julian day (z) + Time of day (sin) + Temperature (z)
8	12	-89687.64	179399.30	1.67	0.08	Species pair + Julian day (z) + Time of day (cos) + Time of day (sin) + Temperature (z)
9	14	-89685.64	179399.30	1.68	0.08	Species pair + Habitat type + Julian day (z) + Slope (z) + Time of day (sin) + Temperature (z)
10	11	-89688.68	179399.40	1.75	0.07	Species pair + Julian day (z) + Time of day (sin) + Temperature (z)
				Cumulative weight		0.18, 0.35, 0.45, 0.54, 0.62, 0.70, 0.78, 0.86, 0.94, 1.00

C.2.3 Roe deer, chamois 1 km

Table C.9: Top models (ΔAICc ≤ 2) used for model averaging for the roe deer, chamois GLMM (1 km). All models include an intercept and random intercepts for *Location* and *Year*; `ziformula = ~0`, `dispformula = ~Habitat type + 1`.

Model	k	logLik	AICc	ΔAICc	Weight	Predictors (fixed effects)
1	11	-12422.56	24867.34	0.00	0.16	Habitat type + Julian day (z) + Precipitation (1h, z) + Temperature (z)
2	10	-12423.67	24867.53	0.19	0.15	Habitat type + Julian day (z) + Temperature (z)
3	12	-12421.91	24868.08	0.74	0.11	Art-pair + Habitat type + Julian day (z) + Precipitation (1h, z) + Temperature (z)
4	11	-12423.01	24868.24	0.90	0.10	Art-pair + Habitat type + Julian day (z) + Temperature (z)
5	12	-12422.23	24868.73	1.39	0.08	Habitat type + Elevation (z) + Julian day (z) + Precipitation (1h, z) + Temperature (z)
6	11	-12423.32	24868.87	1.53	0.07	Habitat type + Elevation (z) + Julian day (z) + Temperature (z)
7	12	-12422.31	24868.88	1.54	0.07	Habitat type + Julian day (z) + Precipitation (1h, z) + Time of day (sin) + Temperature (z)
8	9	-12425.42	24869.00	1.66	0.07	Julian day (z) + Precipitation (1h, z) + Temperature (z)
9	12	-12422.48	24869.22	1.88	0.06	Habitat type + Julian day (z) + Precipitation (1h, z) + Time of day (cos) + Temperature (z)
10	12	-12422.51	24869.29	1.94	0.06	Habitat type + Julian day (z) + Slope (z) + Precipitation (1h, z) + Temperature (z)
11	8	-12426.61	24869.34	1.99	0.06	Julian day (z) + Temperature (z)
				Cumulative weight		0.16, 0.31, 0.42, 0.52, 0.60, 0.67, 0.74, 0.81, 0.87, 0.93, 0.99

C.2.4 Roe deer, chamois 250 m

Table C.10: Top models (ΔAICc ≤ 2) used for model averaging for the roe deer, chamois GLMM (250 m). All models include an intercept and random intercepts for *Location* and *Year*; `ziformula = ~0`, `dispformula = ~Elevation_z + Julian_day_z + 1`.

Model	k	logLik	AICc	ΔAICc	Weight	Predictors (fixed effects)
1	11	-38917.29	77856.65	0.00	0.16	Species pair + Julian day (z) + Slope (z) + Time of day (sin) + Temperature (z)
2	10	-38918.40	77856.86	0.21	0.14	Species pair + Julian day (z) + Slope (z) + Temperature (z)
3	10	-38918.65	77857.35	0.70	0.11	Species pair + Julian day (z) + Time of day (sin) + Temperature (z)
4	9	-38919.77	77857.58	0.93	0.10	Species pair + Julian day (z) + Temperature (z)
5	12	-38916.84	77857.77	1.12	0.09	Species pair + Julian day (z) + Slope (z) + Time of day (cos) + Time of day (sin) + Temperature (z)
6	12	-38916.94	77857.96	1.31	0.08	Species pair + Elevation (z) + Julian day (z) + Slope (z) + Time of day (sin) + Temperature (z)
7	11	-38918.07	77858.21	1.56	0.07	Species pair + Elevation (z) + Julian day (z) + Slope (z) + Temperature (z)

Continued on next page

Model	k	logLik	AICc	ΔAICc	Weight	Predictors (fixed effects)
8	12	-38917.12	77858.32	1.67	0.07	Species pair + Julian day (z) + Slope (z) + Precipitation (1h, z) + Time of day (sin) + Temperature (z)
9	11	-38918.17	77858.42	1.76	0.06	Species pair + Elevation (z) + Julian day (z) + Time of day (sin) + Temperature (z)
10	11	-38918.20	77858.47	1.82	0.06	Species pair + Julian day (z) + Time of day (cos) + Time of day (sin) + Temperature (z)
11	11	-38918.25	77858.58	1.92	0.06	Species pair + Julian day (z) + Slope (z) + Time of day (cos) + Temperature (z)
				Cumulative weight		0.16, 0.30, 0.41, 0.51, 0.60, 0.68, 0.75, 0.82, 0.88, 0.94, 1.00

C.2.5 Chamois, red deer 1 km

Table C.11: Top models (ΔAICc ≤ 2) used for model averaging for the chamois, red deer GLMM (1 km). All models include an intercept and random intercepts for *Location* and *Year*; `ziformula = ~0`, `dispformula = ~Elevation_z + Julian_day_z + 1`.

Model	k	logLik	AICc	ΔAICc	Weight	Predictors (fixed effects)
1	13	-78966.19	157958.40	0.00	0.45	Species pair + Habitat type + Julian day (z) + Time of day (cos) + Time of day (sin) + Temperature (z)
2	14	-78965.99	157960.00	1.60	0.20	Species pair + Habitat type + Elevation (z) + Julian day (z) + Time of day (cos) + Time of day (sin) + Temperature (z)
3	12	-78968.08	157960.20	1.77	0.19	Species pair + Habitat type + Julian day (z) + Time of day (sin) + Temperature (z)
4	14	-78966.18	157960.40	2.00	0.17	Species pair + Habitat type + Julian day (z) + Precipitation (1h, z) + Time of day (cos) + Time of day (sin) + Temperature (z)
				Cumulative weight		0.45, 0.65, 0.84, 1.00